

States of the ^{12}C Nucleus in the Toroidal Configuration

Cheuk-Yin Wong*

Physics Division, Oak Ridge National Laboratory, Oak Ridge, TN 37831, USA

Andrzej Staszczak†

*Institute of Physics, Maria Curie-Skłodowska University,
pl. M. Curie-Skłodowskiej 1, 20-031 Lublin, Poland*

(Dated: December 15, 2024)

The ^{12}C nucleus with $N=6$ and $Z=6$ is a doubly-magic closed-shell nucleus in a toroidal potential and Wheeler's triangular resonating group model of ^{12}C as three clusters of alpha particles will naturally generate a toroidal density if the nucleons interchanging between the clusters are allowed to circulate continuously from one cluster to another. Experimentally, many excited states of ^{12}C decay predominantly into three alpha particles, and the triangular clusters of three alpha particles have a high degree of overlap with a torus. We explore a toroidal description for some excited states of ^{12}C and search for the signature that will reveal a possible toroidal configuration of the nucleus. We find that the ^{12}C nucleus in a toroidal configuration distinguishes itself by toroidal multiplets of particle-hole excitations between one toroidal shell to another. Subject to further confirmation, the Hoyle state and many of its higher excited states may be tentatively attributed to those of a ^{12}C nucleus in a toroidal configuration.

PACS numbers: 21.10.Pc, 21.60.Cs

I. INTRODUCTION

The study of the intrinsic structure of the ^{12}C nucleus has a long history. Wheeler proposed an α particle model for α -conjugate nuclei and suggested in 1937 that the ^{12}C nucleus may be described as a triangular resonating grouping of three alpha clusters obeying Bose-Einstein statistics and exchanging nucleons between them [1, 2]. Later in 1953 Hoyle postulated an excited state of ^{12}C as the doorway for the triplet alpha reaction in nucleosynthesis, in which two alpha particles fuse into beryllium-8 and then capture a third alpha particle to form the carbon-12 element [3–5]. The excited 0^+ state at 7.654 MeV of ^{12}C was subsequently identified as the postulated “Hoyle state” [6]. Since then, many experimental and theoretical investigations have been carried out to understand the properties of the ^{12}C nucleus. Recent experimental results and related reviews have been presented in [7–17]. In addition to Wheeler's α particle model, related theoretical models include the cluster model of Brink [18], an interacting cluster model of three alpha particles [19–21], a Nilsson oblate ellipsoidal model [22] with a commensurate axis ratio [23], an algebraic $U(7)$ model with a D_{3h} symmetry [24, 25], an antisymmetric molecular dynamics (AMD) model [26–28], a microscopic fermionic molecular dynamic (FMD) model [29, 30], a Bose-Einstein condensate-type cluster model [31], an *ab initio* no-core shell model [32, 33], a no-core symplectic model (NCSpm) [34], *ab initio* lattice effective field theory (L-EFT) [35], microscopic cluster models [36], energy-density functional mean-field models

[37–44], and a rod model of excited states [45–47].

We explore here an additional toroidal model of the ^{12}C nucleus for many reasons. First and foremost is the reason that the nature of many excited states of ^{12}C has not been fully understood [7–17]. On the other hand, in the single-particle energy level diagram for a toroidal nucleus [48, 49], the ^{12}C nucleus with $N=6$ and $Z=6$ is a doubly-magic closed-shell nucleus. Toroidal excited states have been predicted in the mass region of $40 \leq A \leq 70$ [48, 49] by employing the shell-correction method [50]. The extrapolation from these results points to a possible toroidal local equilibrium in ^{12}C in the low excitation energy region. Furthermore, recent experimental observation of narrow resonances in excited ^{28}Si [51] suggests possible population of toroidal high-spin isomers as predicted previously in ^{28}Si [52]. Similar toroidal high-spin isomers have also been predicted in the light-mass region from ^{24}Mg to ^{56}Ni in relativistic and non-relativistic mean-field theories [52–58]. It is also interesting to note that Wheeler's triangular resonating group model of the ^{12}C nucleus with the D_{3h} symmetry [24, 25] represents a model of three quasi-static clusters with the interchange of nucleons between them. In a more general dynamical description, if the nucleons interchanging between the triangular clusters are allowed to circulate continuously and self-consistently from one cluster to another, they will generate naturally a toroidal density distribution. Experimentally, many excited states of ^{12}C decay predominantly into three alpha particles [13–17], and a triangular cluster of three alpha particles has a high degree of overlap with a torus. For all these reasons, it is of interest to explore whether some excited states of the ^{12}C nucleus may be attributed to those of the nucleus in a toroidal configuration.

The band of 0^+ (ground) and 2^+ (4.33 MeV) states of

* wongc@ornl.gov

† andrzej.staszczak@poczta.umcs.lublin.pl

the ^{12}C nucleus have been identified as collective states of an oblate spheroid with $\beta = -0.6$ [59]. Toroidal states of ^{12}C , if exist, can only be associated with higher excited states of ^{12}C above the 2^+ (4.33 MeV) state. The next higher excited state is the 0^+ Hoyle state at 7.654 MeV, which decays predominantly into three alpha particles. Since the triangular clusters of three alpha particles have a large overlap with a toroidal distribution, the Hoyle state presents itself as a good candidate to be a member of the toroidal states of ^{12}C . Because the toroidal configuration and the oblate spheroid configuration have distinct topologies, the toroidal states and the oblate spheroid states are likely to be independent without substantial mixing, if they co-exist in ^{12}C .

The intrinsic shape of a ^{12}C nucleus in the toroidal configuration shows up as a distinct spectrum of a set of states that are intimately tied to each other through its toroidal geometry. Such a distinct spectrum of states constitute the toroidal signature that will reveals a possible toroidal configuration of the nucleus. We shall look for such a signature among the excited states of ^{12}C and explore whether the Hoyle state at 7.654 MeV may be the ground state of the toroidal band of the ^{12}C nucleus. By comparison with experimental data, we find that subject to further confirmation, the Hoyle state and many of its higher excited states may be tentatively attributed to those of a ^{12}C nucleus in a toroidal configuration.

The paper is organized as follows. In Section II, we write down the single-particle state energies of a toroidal nucleus in the approximation of a large major radius with the neglect of the small spin orbit interaction. They depend only on the toroidal major radius R and the orbital angular momentum component Λ_z along the symmetry z -axis. The method to calculate the quantum numbers and the excitation energies of the particle-hole excitations from these single-particle states are examined in Section III. The spectrum of ^{12}C in the toroidal configuration is investigated in Section IV with the details of the calculations for higher excited states included in the Appendix. In Section V, we confront the theoretical predicted spectrum of toroidal states with observed ^{12}C spectrum. We find tentatively that the Hoyle state and many of its higher states may be attributed to those of a ^{12}C nucleus in a toroidal configuration. In Section VI, we propose a toroidal constraint in mean-field dynamics to study the energy surface in the toroidal degree of freedom and to locate local energy minima in the toroidal configuration. In Section VII, we present our summary and discussions.

II. SINGLE-PARTICLE STATES IN A TOROIDAL POTENTIAL

Nucleons in a toroidal nucleus generate a mean-field potential that has the same shape as the toroidal density distribution. To get the spectrum of a toroidal nucleus, we place the nucleons in the lowest states in

the toroidal potential, make the single-particle particle-hole excitations, and record their excitation energies and quantum numbers. The single-particle potential can be represented by a toroidal harmonic oscillator potential with minima at $\rho=R$ and $z=0$ in cylindrical coordinates (ρ, z, ϕ) [48, 49]

$$V_0(\rho, z) = \frac{1}{2}m\omega_\perp^2 \{(\rho - R)^2 + z^2\}, \quad (1)$$

where $\rho = \sqrt{x^2 + y^2}$, the symmetry axis lies along the z -direction, ω_\perp is the harmonic oscillator frequency, and m is the rest mass of a nucleon. By introducing the radial difference $q = \rho - R$, we re-write the above potential as

$$V_0(\rho, z) = \frac{1}{2}m\omega_\perp^2 (q^2 + z^2). \quad (2)$$

Approximate analytical solutions of the single-particle eigenenergies have been obtained by making the large major radius approximation, in which the major radius R is much greater than the minor radius d [60]. In that approximation, the variable q can be extended to $-\infty$ without serious errors so that the above potential (2) is just a two-dimensional simple harmonic oscillator potential in q and z . The eigenstates are labeled by $|n_\rho n_z \Lambda_z \Omega_z\rangle$, where n_ρ and n_z are the harmonic oscillator quantum numbers of the potential (2), Ω_z is $\Lambda_z + s_z$, Λ_z is the orbital angular momentum component Λ_z , and s_z is the intrinsic spin component. The single-particle energies are given approximately by [60]

$$\begin{aligned} \epsilon(n_\rho n_z \Lambda_z \Omega_z) = & (n_\rho + \frac{1}{2})\hbar\omega'_\perp + (n_z + \frac{1}{2})\hbar\omega_\perp \\ & + \frac{\hbar^2}{2m} \frac{\Lambda_z^2 - \frac{1}{4}}{R^2} + a_0, \end{aligned} \quad (3)$$

where

$$\omega'^2_\perp = \omega_\perp^2 (1 + a_2), \quad (4)$$

$$a_2 = \frac{1}{m\omega_\perp^2} \left\{ \frac{\hbar^2}{2m} \frac{\Lambda_z^2 - \frac{1}{4}}{R^2} \frac{6}{R^2} + \frac{2\kappa(\hbar\omega_\perp)^2}{\hbar\omega_0} s_z \Lambda_z \frac{2}{R^2} \right\}, \quad (5)$$

$$\begin{aligned} a_0 = & \frac{1}{2}m\omega_\perp^2 q_0^2 + \frac{\hbar^2}{2m} \frac{\Lambda_z^2 - \frac{1}{4}}{R^2} \left(-\frac{2q_0}{R} + \frac{3q_0^2}{R^2} \right) \\ & - \frac{2\kappa(\hbar\omega_\perp)^2}{\hbar\omega_0} s_z \Lambda_z \left(\frac{q_0}{R} - \frac{q_0^2}{R^2} \right), \end{aligned} \quad (6)$$

$$q_0 = \frac{1}{m\omega_\perp^2 (1 + a_2)} \left\{ \frac{\hbar^2}{2m} \frac{\Lambda_z^2 - \frac{1}{4}}{R^2} \frac{2}{R} + \frac{2\kappa(\hbar\omega_\perp)^2}{\hbar\omega_0} \frac{s_z \Lambda_z}{R} \right\}, \quad (7)$$

where κ is the strength of the spin-orbit interaction [22] and $\hbar\omega_0$ is the harmonic oscillator constant of an equivalent spherical nucleus with the same volume [61]

$$\hbar\omega_0 = 41 \text{ MeV}/A^{1/3}. \quad (8)$$

We shall limit our attention only to low-lying excited states involving nucleons with $n_\rho=0$ and $n_z=0$ and the lowest few Λ_z . For convenience of notation, we shall omit

n_ρ and n_z from the state labels. The nuclear spin unit \hbar will be implicitly understood. Upon neglecting further the small spin-orbit splitting for these single-particle states with $n_\rho=0$ and $n_z=0$, the single-particle energies are given approximately by

$$\epsilon(\Lambda_z \Omega_z) \equiv \epsilon(n_\rho=0, n_z=0, \Lambda_z \Omega_z) \approx \frac{\hbar^2}{2m} \frac{\Lambda_z^2 - \frac{1}{4}}{R^2} + \hbar \omega_\perp. \quad (9)$$

III. PARTICLE-HOLE EXCITATIONS OF A CLOSED SHELL TOROIDAL NUCLEUS

The density of single-particle states in the energy space is far from being uniform in a toroidal nucleus. With the single-particle state energies given by Eq. (3) or (9) for a toroidal nucleus, the single-particle state energies cluster together into “shells” in the single-particle energy space, with a large energy gap between one shell and the next, generating magic numbers $N = 2(2m + 1)$ with integer $m \geq 1$ in the light-mass region [48, 49, 60]. There, the toroidal shells can be labeled as “ Λ_z -shells”, where Λ_z is the orbital angular momentum component of the states in the shell, as shown schematically in Fig. 1. The toroidal ground state of the ^{12}C nucleus with the closed toroidal shells is described by nucleons occupying the $\Lambda_z=0$ and $\Lambda_z=1$ toroidal shells, filling up the lowest single-particle states of $|0 \pm \frac{1}{2}\rangle$, $|1 \pm \frac{1}{2}\rangle$, $|1 \pm \frac{3}{2}\rangle$, as in Fig. 1.

The doubly-magic nature of the ^{12}C nucleus in the toroidal configuration means that the energy gap between the occupied states in the $\Lambda_z=1$ shell and the unoccupied states in the $\Lambda_z=2$ shell is expected to be quite large, presumably much larger than the spin-orbit and residual interactions. Thus, the single-particle particle-hole excitations will yield the gross structure, while the spin-orbit and residual interactions will provide the fine structure of the spectrum. In the present first survey we shall contend ourselves only with the gross structure by studying particle-hole excitations built on toroidal single-particle shells without spin-orbit and residual interactions. Refinement of the energy spectrum can be carried out in the projected shell model calculations using the toroidal states as basis states as in [62–65].

We use the single-particle energies Eq. (9) to evaluate the energy spectrum of a double-closed shell toroidal nucleus by calculating the particle-hole excitation energy $E_I - E_0$ and its associated angular momentum component I_z , at the equilibrium toroidal major radius R . We call the angular momentum component I_z along the symmetry axis with $I_z=I$ the spin I (or I_z) of the toroidal state.

The multiplet of (n particle)-(n hole) excitations from the ground state constructed by promoting n nucleons from the occupied Λ_{zi} shell to the empty Λ_{zf} shell will be labeled as $(\text{nph})_{\Lambda_{zi}\Lambda_{zf}}^\pi$, where π , the parity of the multiplet, is equal to $(-1)^{\Lambda_{zf}-\Lambda_{zi}}$. In particular, the $(1\text{p}1\text{h})_{\Lambda_{zi}\Lambda_{zf}}^\pi$ multiplet of particle-hole excitations can be constructed by promoting a nucleon from an occupied

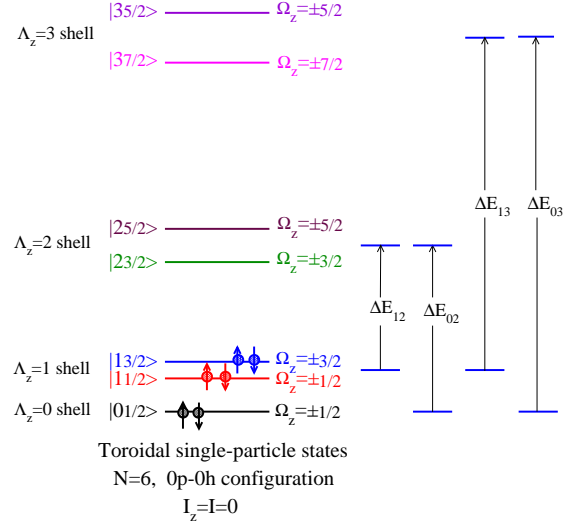


FIG. 1. (Colour online.) Schematic toroidal single-particle energy level diagram for neutrons or protons, with the nucleons occupying the lowest single-particle states for the ^{12}C nucleus in the toroidal configuration. The excitation energies $\Delta E_{\Lambda_{zi}\Lambda_{zf}}$ for various 1p1h excitations from the Λ_{zi} toroidal shell to the Λ_{zf} toroidal shell are schematically indicated.

initial state $|\Lambda_z \Omega_z\rangle_i$ in the Λ_{zi} shell to an unoccupied final state $|\Lambda_z \Omega_z\rangle_f$ in the Λ_{zf} shell. From Eq. (9), such a particle-hole excitation leads to a spin increment $\Delta_{if} I_z$ for such an $\{i \rightarrow f\}$ particle-hole excitation given by

$$\Delta_{if} I_z([\Lambda_z \Omega_z]_i \rightarrow [\Lambda_z \Omega_z]_f) = \Omega_{zf} - \Omega_{zi}, \quad (10)$$

and an excitation energy increment $\Delta_{if} E_{\Lambda_i \Lambda_f}$ given by

$$\begin{aligned} \Delta_{if} E_{\Lambda_i \Lambda_f}([\Lambda_z \Omega_z]_i \rightarrow [\Lambda_z \Omega_z]_f) &= \epsilon([\Lambda_z \Omega_z]_f) - \epsilon([\Lambda_z \Omega_z]_i) \\ &= \frac{\hbar^2}{2mR^2} (\Lambda_{zf}^2 - \Lambda_{zi}^2). \end{aligned} \quad (11)$$

Here the energy unit $\hbar^2/2mR^2$ appears so frequently in the excitation energy expressions that it deserves a symbol of its own. We call it ϵ_0 ,

$$\epsilon_0 = \frac{\hbar^2}{2mR^2}. \quad (12)$$

The spin I_z and excitation energy E_x of a state in the $(\text{nph})_{\Lambda_{zi}\Lambda_{zf}}^\pi$ multiplet, in the simplest approximation with the neglect of spin-orbit and residual interactions, are just additive sums of the spin and energy increments from independent $\{i \rightarrow f\}$ particle-hole excitations, subject to the Pauli exclusion principle,

$$I_z = \sum_{if} \Delta_{if}([\Lambda_z \Omega_z]_i \rightarrow [\Lambda_z \Omega_z]_f). \quad (13)$$

The parity π of the state is

$$\pi = \prod_{if} \{(-1)^{\Lambda_{zf}-\Lambda_{zi}}\}. \quad (14)$$

Because there are many different Ω_z states in a single-particle Λ_z shell, there are many different spin increments in an $(\text{nph})_{\Lambda_z i \Lambda_z f}^\pi$ multiplet. Consequently there are many different I_z spins in the multiplet states of the toroidal nucleus. All these states with different spins $I = I_z$ within the multiplet have the same parity π and are degenerate with the excitation energy

$$E_x = E_I - E_0 = \sum_{if} \Delta_{if} E_{\Lambda_i \Lambda_f} ([\Lambda_z \Omega_z]_i \rightarrow [\Lambda_z \Omega_z]_f), \quad (15)$$

where E_0 is the energy of the toroidal ground state relative to the ^{12}C ground state. The inclusion of spin-orbit and residual interactions in a more refined calculation will split the degeneracy of the different I_z states in the multiplet.

IV. SPECTRUM OF THE ^{12}C NUCLEUS IN THE TOROIDAL CONFIGURATION

In this section, we shall show explicitly how the spectrum of the low-lying toroidal ^{12}C can be determined from the toroidal single-particle energies. We shall include the determination of higher ^{12}C toroidal states in the Appendix.

A. $(1p1h)_{\Lambda_z i \Lambda_z f}^\pi$ Toroidal States

As one can see from Fig. 1, different $(1p1h)_{\Lambda_z i \Lambda_z f}^\pi$ multiplets of excited ^{12}C toroidal states arise by promoting nucleons from $\{[0(\pm 1/2)], [1(\pm 1/2)], [1(\pm 3/2)]\}$ toroidal states in the $\Lambda_z=0$ and 1 shells to occupy empty $\{[2(\pm 5/2)], [2(\pm 3/2)], [3(\pm 7/2)], [3(\pm 5/2)]\}$ toroidal states in the $\Lambda_z=2$ and 3 shells. The knowledge of the particle and hole state quantum numbers gives the spin and parity of the excitation, and the excitation energy can be determined from the single-particle energy (9) or the energy increment (15). In particular, for a member I_z^π with $I = I_z$ in the $(1p1h)_{\Lambda_z i \Lambda_z f}^\pi$ multiplet, the energy E_I of the member relative to the toroidal ground state of energy E_0 is given by

$$E_I - E_0 = \Delta E_{\Lambda_z i \Lambda_z f}. \quad (16)$$

All members of a multiplet have the same excitation energy in the present idealized approximation with the neglect of the spin-orbit and residual interactions.

The (one particle)-(one hole) $\Delta E_{\Lambda_z i \Lambda_z f}$ for different shell-to-shell excitations are

$$\begin{aligned} \Delta E_{12} &= \epsilon(|\Lambda_z| = 1) \rightarrow \epsilon(|\Lambda_z| = 2) = \frac{3\hbar^2}{2mR^2} = 3\epsilon_0, \\ \Delta E_{02} &= \epsilon(|\Lambda_z| = 0) \rightarrow \epsilon(|\Lambda_z| = 2) = \frac{4\hbar^2}{2mR^2} = 4\epsilon_0, \\ \Delta E_{13} &= \epsilon(|\Lambda_z| = 1) \rightarrow \epsilon(|\Lambda_z| = 3) = \frac{8\hbar^2}{2mR^2} = 8\epsilon_0, \\ \Delta E_{03} &= \epsilon(|\Lambda_z| = 0) \rightarrow \epsilon(|\Lambda_z| = 3) = \frac{9\hbar^2}{2mR^2} = 9\epsilon_0. \end{aligned} \quad (17)$$

These excitation energies depend only on a single-parameter, the major radius R , which can be determined by confronting the predicted theoretical spectrum with the experimental data in the next Section.

The parity of a member I_z^π member of the $(1p1h)_{\Lambda_z i \Lambda_z f}^\pi$ multiplet, is

$$\pi = (-1)^{\Lambda_{zf} - \Lambda_{zi}}. \quad (18)$$

TABLE I. The $(1p1h)_{\Lambda_z i \Lambda_z f}^\pi$ excitations in toroidal ^{12}C where $[\Lambda_{zf} \Omega_{zf}]$ represents a particle state and $[\Lambda_{zi} \Omega_{zi}]^{-1}$ represents the hole state.

particle-hole excitation	particle-hole configuration	I_z^π	$\frac{E_I - E_0}{\epsilon_0}$
$(1p1h)_{12}^-$ $\Lambda_z=1$ shell $\rightarrow \Lambda_z=2$ shell	$[1(-3/2)]^{-1} [2(5/2)]$	4^-	3
	$[1(-1/2)]^{-1} [2(5/2)]$	3^-	
	$[1(1/2)]^{-1} [2(5/2)]$	2^-	
	$[1(3/2)]^{-1} [2(5/2)]$	1^-	
	$[1(-3/2)]^{-1} [2(3/2)]$	3^-	
	$[1(-1/2)]^{-1} [2(3/2)]$	2^-	
	$[1(1/2)]^{-1} [2(3/2)]$	1^-	
	$[1(3/2)]^{-1} [2(3/2)]$	0^-	
$(1p1h)_{02}^+$ $\Lambda_z=0$ shell $\rightarrow \Lambda_z=2$ shell	$[0(-1/2)]^{-1} [2(5/2)]$	3^+	4
	$[0(1/2)]^{-1} [2(5/2)]$	2^+	
	$[0(-1/2)]^{-1} [2(3/2)]$	2^+	
	$[0(1/2)]^{-1} [2(3/2)]$	1^+	
$(1p1h)_{13}^+$ $\Lambda_z=1$ shell $\rightarrow \Lambda_z=3$ shell	$[1(-3/2)]^{-1} [3(7/2)]$	5^+	8
	$[1(-1/2)]^{-1} [3(7/2)]$	4^+	
	$[1(1/2)]^{-1} [3(7/2)]$	3^+	
	$[1(3/2)]^{-1} [3(7/2)]$	2^+	
	$[1(-3/2)]^{-1} [3(5/2)]$	4^+	
	$[1(-1/2)]^{-1} [3(5/2)]$	3^+	
	$[1(1/2)]^{-1} [3(5/2)]$	2^+	
	$[1(3/2)]^{-1} [3(5/2)]$	1^+	
$(1p1h)_{03}^-$ $\Lambda_z=0$ shell $\rightarrow \Lambda_z=3$ shell	$[0(-1/2)]^{-1} [3(7/2)]$	4^-	9
	$[0(1/2)]^{-1} [3(7/2)]$	3^-	
	$[0(-1/2)]^{-1} [3(5/2)]$	3^-	
	$[0(1/2)]^{-1} [3(5/2)]$	2^-	

We show the spin quantum number I_z , parity π , and the excitation energy $E_I - E_0$ of different $(1p1h)_{\Lambda_z i \Lambda_z f}^\pi$ multiplets of excited toroidal states in Table I. We have kept the sign of Ω_z of the particle state positive. If we study the remaining case by reversing the sign of Ω_z of the particle state, we obtain the same set of states as in Table I, except that the signs of I_z is reversed if it is non-zero, and it has a different particle-hole combination if I_z is zero. Thus, each of the total set of states in Table I is doubly degenerate. The double degeneracy occurs repeatedly in all toroidal states, and we shall make its double degeneracy implicit and shall consider only non-negative values of I_z with double degeneracy in what follows, unless explicitly specified otherwise. Furthermore, it should be kept in mind that Table I is applicable to neutron as well as to proton $(1p1h)$ excitations.

Table I and Fig. 2 show that the $(1p1h)_{12}^\pi$ multiplet for the excitation of a nucleon from the $\Lambda_z=1$ shell

to the $\Lambda_z=2$ shell consists of a set of eight doubly-degenerate states, $\{4^-, 2(3^-), 2(2^-), 2(1^-), 0^-\}$, lying at $E_x = E_I - E_0 = 3\epsilon_0$. The $(1p1h)_{02}^+$ multiplet for the excitation of a nucleon from the $\Lambda_z=0$ shell to the $\Lambda_z=2$ shell consists of a set of four states, $\{(3^+), 2(2^+), 1^+\}$, lying at an excitation energy $E_x = 4\epsilon_0$. The $(1p1h)_{13}^+$ multiplet for the excitation of a nucleon from the $\Lambda_z=1$ shell to the $\Lambda_z=3$ shell consists of a set of eight states of $\{5^+, 2(4^+), 2(3^+), 2(2^+), 1^+\}$ lying at $E_x = 8\epsilon_0$. Finally, the $(1p1h)_{03}^-$ multiplet for the excitation of a nucleon from the $\Lambda_z=0$ shell to the $\Lambda_z=3$ shell consists of a set of four doubly-degenerate states, $\{(4^-), 2(3^-), 2^-\}$, lying at $E_x = 9\epsilon_0$. The spectrum of these states are shown in Fig. 2.

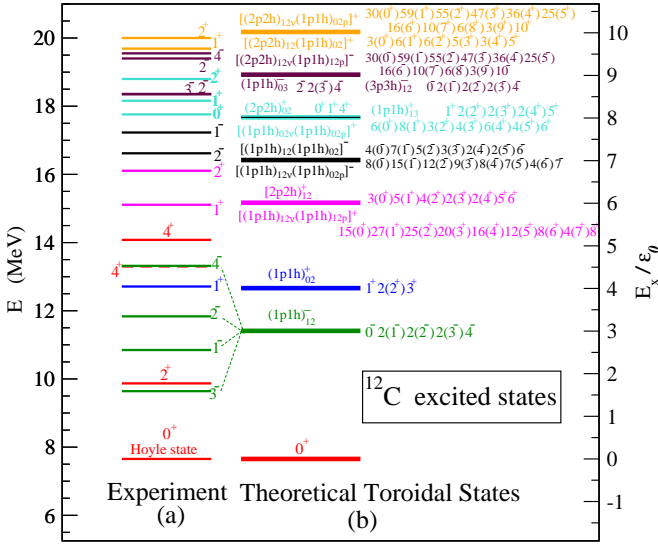


FIG. 2. (Colour online.) (a) Experimental excitation energy E of ^{12}C excited states relative to the ^{12}C ground state [13], with the axis of the excitation energy E on the left. (b) The theoretical spectrum of the toroidal states in different multiplets, with the axis of the excitation energy $E_x = E - E_0$, relative to the energy E_0 of the toroidal ground state, given on the right. Comparison between the experimental and theoretical spectra is made by identifying the Hoyle state as the toroidal ground state and the lowest lying $3^-, 1^-, 2^-, 4^-$ as members of the toroidal $(1p1h)_{12}^-$ multiplet, leading to $\epsilon_0 = 1.25$ MeV (see text). The spins and parities of members of the multiplets are presented in the figure and given in Table VI.

The lowest lying toroidal states are the $(1p1h)_{12}^-$ and $(1p1h)_{02}^+$ multiplets lying above the ground toroidal ^{12}C state. They should be prominently excited by stripping ($^3\text{He}, d$) reactions that add a proton to excite and combine with a ^{11}B nucleus to a toroidal configuration.

B. $[(2p2h)_{12}]^+$ at $E_x = 6\epsilon_0$ for exciting two identical nucleons from $\Lambda_z=1$ shell to $\Lambda_z=2$ shell

We consider next the $(2p2h)_{12}^+$ excitations of two identical particles (neutrons or protons) from the $\Lambda_z=1$ shell to the $\Lambda_z=2$ shell. Because of the Pauli exclusion principle, the two identical particle or holes cannot occupy the same $|\Lambda_z, \Omega_z\rangle$ state. Consequently, to get the (2 particle)-(2 hole) excitations involving identical particles, it is simplest to combine the angular momentum components of the two particles and two holes separately first, under the restriction of the Pauli principle, before combining them together. For this purpose, we list all combinations of states of two holes in Table II and two particles in Table III, under the restriction of the Pauli principle.

TABLE II. Combination of two holes states in $|1(\pm 3/2)\rangle$ and $|1(\pm 1/2)\rangle$ states in the $\Lambda_z=1$ shell under the restriction of the Pauli principle

two hole configuration	I_z^π
$\{ 1(3/2)\rangle[1(1/2)]\}^{-1}$	$[2^+]^{-1}$
$\{ 1(3/2)\rangle[1(-1/2)]\}^{-1}$	$[1^+]^{-1}$
$\{ 1(1/2)\rangle[1(-1/2)]\}^{-1}$	$[0^+]^{-1}$
$\{ 1(-3/2)\rangle[1(3/2)]\}^{-1}$	$[0^+]^{-1}$
$\{ 1(-3/2)\rangle[1(1/2)]\}^{-1}$	$[(-1)^+]^{-1}$
$\{ 1(-3/2)\rangle[1(-1/2)]\}^{-1}$	$[(-2)^+]^{-1}$

TABLE III. Combination of two particles states in $|2 \pm 5/2\rangle$ and $|2 \pm 3/2\rangle$ orbitals in the $\Lambda_z=2$ shell under the restriction of the Pauli principle

two particle configuration	I_z^π
$\{[2(5/2)][2(3/2)]\}$	4^+
$\{[2(5/2)][2(-3/2)]\}$	1^+
$\{[2(3/2)][2(-3/2)]\}$	0^+
$\{[2(-5/2)][2(5/2)]\}$	0^+
$\{[2(-5/2)][2(3/2)]\}$	$(-1)^+$
$\{[2(-5/2)][2(-3/2)]\}$	$(-4)^+$

Now combine the two hole states with all two particle states, we get the angular momentum component I_z and parity π as listed in Table IV. As one observes in Table IV, the $(2p2h)_{12}^+$ multiplet consists of a set of 18 doubly-degenerate positive parity states, $\{6^+, 5^+, 2(4^+), 2(3^+), 4(2^+), 5(1^+), 3(0^+)\}$, lying at $E_x = 6\epsilon_0$ as shown in Fig. 2(b). It is applicable to a pair of neutrons or protons.

TABLE IV. The spin states of the $(2p2h)_{12}^+$ multiplet at $E_x=6\epsilon_0$ for the excitation of two identical nucleons from the $\Lambda_z=1$ shell to the $\Lambda_z=2$ shell

two holes	two particle configuration	I_z^π
$\{[1(3/2)][1(1/2)]\}^{-1}$	$\{[2(5/2)][2(3/2)]\}$	2^+
	$\{[2(5/2)][2(-3/2)]\}$	$(-1)^+$
	$\{[2(3/2)][2(-3/2)]\}$	$(-2)^+$
	$\{[2(-5/2)][2(5/2)]\}$	$(-2)^+$
	$\{[2(-5/2)][2(3/2)]\}$	$(-3)^+$
	$\{[2(-5/2)][2(-3/2)]\}$	$(-6)^+$
$\{[1(3/2)][1(-1/2)]\}^{-1}$	$\{[2(5/2)][2(3/2)]\}$	3^+
	$\{[2(5/2)][2(-3/2)]\}$	0^+
	$\{[2(3/2)][2(-3/2)]\}$	$(-1)^+$
	$\{[2(-5/2)][2(5/2)]\}$	$(-1)^+$
	$\{[2(-5/2)][2(3/2)]\}$	$(-2)^+$
	$\{[2(-5/2)][2(-3/2)]\}$	$(-5)^+$
$\{[1(1/2)][1(-1/2)]\}^{-1}$	$\{[2(5/2)][2(3/2)]\}$	4^+
	$\{[2(5/2)][2(-3/2)]\}$	1^+
	$\{[2(3/2)][2(-3/2)]\}$	0^+
	$\{[2(-5/2)][2(5/2)]\}$	0^+
	$\{[2(-5/2)][2(3/2)]\}$	$(-1)^+$
	$\{[2(-5/2)][2(-3/2)]\}$	$(-4)^+$
$\{[1(-3/2)][1(3/2)]\}^{-1}$	$\{[2(5/2)][2(3/2)]\}$	4^+
	$\{[2(5/2)][2(-3/2)]\}$	1^+
	$\{[2(3/2)][2(-3/2)]\}$	0^+
	$\{[2(-5/2)][2(5/2)]\}$	0^+
	$\{[2(-5/2)][2(3/2)]\}$	$(-1)^+$
	$\{[2(-5/2)][2(-3/2)]\}$	$(-4)^+$
$\{[1(-3/2)][1(1/2)]\}^{-1}$	$\{[2(5/2)][2(3/2)]\}$	5^+
	$\{[2(5/2)][2(-3/2)]\}$	2^+
	$\{[2(3/2)][2(-3/2)]\}$	1^+
	$\{[2(-5/2)][2(5/2)]\}$	1^+
	$\{[2(-5/2)][2(3/2)]\}$	0^+
	$\{[2(-5/2)][2(-3/2)]\}$	$(-3)^+$
$\{[1(-3/2)][1(-1/2)]\}^{-1}$	$\{[2(5/2)][2(3/2)]\}$	6^+
	$\{[2(5/2)][2(-3/2)]\}$	3^+
	$\{[2(3/2)][2(-3/2)]\}$	2^+
	$\{[2(-5/2)][2(5/2)]\}$	2^+
	$\{[2(-5/2)][2(3/2)]\}$	1^+
	$\{[2(-5/2)][2(-3/2)]\}$	$(-2)^+$

C. $[(1p1h)_{12\nu}(1p-1h)_{12p}]^+$ toroidal multiplet involving one neutron and one proton

In the last subsection, we have considered the $(2p2h)$ excitations involving two identical nucleons. The case of the $(2p2h)$ excitations involving two different types of nucleons from the $\Lambda_z = 1$ shell to the $\Lambda_z = 2$ shell differ from the previous case, because the pairs of particles or holes do not need to be restricted by the Pauli principle. We can consider such $(2p-2h)$ excitations by combining a $(1p1h)$ neutron excitation with an independent $(1p1h)$ proton excitation. Such a $[(1p1h)_{12\nu}(1p-1h)_{12p}]^\pi$ multiplet has the excitation energy $E_x = 2\Delta E_{12} = 6\epsilon_0$ and positive parity. Their spin quantum numbers I_z and parities

are given in Table V.

TABLE V. The spin states of the $[(1p1h)_{12\nu}(1p1h)_{12p}]^+$ multiplet at $E_x=6\epsilon_0$ involving different types of nucleons

$(1p1h)_{12\nu}$ State	$(1p1h)_{12p}$ State							
	4^-	3^-	2^-	1^-	3^-	2^-	1^-	0^-
4^-	8^+	7^+	6^+	5^+	7^+	6^+	5^+	4^+
3^-	7^+	6^+	5^+	4^+	6^+	5^+	4^+	3^+
2^-	6^+	5^+	4^+	3^+	5^+	4^+	3^+	2^+
1^-	5^+	4^+	3^+	2^+	4^+	3^+	2^+	1^+
3^-	7^+	6^+	5^+	4^+	6^+	5^+	4^+	3^+
2^-	6^+	5^+	4^+	3^+	5^+	4^+	3^+	2^+
1^-	5^+	4^+	3^+	2^+	4^+	3^+	2^+	1^+
0^-	4^+	3^+	2^+	1^+	3^+	2^+	1^+	0^+
$(-4)^-$	0^+	$(-1)^+$	$(-2)^+$	$(-3)^+$	$(-1)^+$	$(-2)^+$	$(-3)^+$	$(-4)^+$
$(-3)^-$	1^+	0^+	$(-1)^+$	$(-2)^+$	0^+	$(-1)^+$	$(-2)^+$	$(-3)^+$
$(-2)^-$	2^+	1^+	0^+	$(-1)^+$	1^+	0^+	$(-1)^+$	$(-2)^+$
$(-1)^-$	3^+	2^+	1^+	0^+	2^+	1^+	0^+	$(-1)^+$
$(-3)^-$	1^+	0^+	$(-1)^+$	$(-2)^+$	0^+	$(-1)^+$	$(-2)^+$	$(-3)^+$
$(-2)^-$	2^+	1^+	0^+	$(-1)^+$	$(-2)^+$	0^+	$(-1)^+$	$(-2)^+$
$(-1)^-$	3^+	2^+	1^+	0^+	2^+	1^+	0^+	$(-1)^+$
0^-	4^+	3^+	2^+	1^+	3^+	2^+	1^+	0^+

There are altogether $\{8^+, 4(7^+), 8(6^+), 12(5^+), 15(4^+), 16(3^+), 16(2^+), 15(1^+), 15(0^+), 1(-4)^+, 4(-3)^+, 9(-2)^+, 12(-1)^+\}$ for a total of 128 states. If we reverse the sign of the $(1p1h)_{12p}$ state, we get the same set of states but with the signs of I_z is reversed if it is non-zero, and it has a different particle-hole combination if I_z is zero. The $(I_z)^+$ and the $(-I_z)^+$ states in these two sets can be grouped together. In this new grouping, the combined set contains 128 doubly-degenerate states of the set $\{8^+, 4(7^+), 8(6^+), 12(5^+), 16(4^+), 20(3^+), 25(2^+), 27(1^+), 15(0^+)\}$ at the excitation energy $E_x = 2\Delta E_{12} = 6\epsilon_0$.

We have thus obtained the spectrum of the lowest-lying multiplets of states. The spectrum of the higher states are included in the Appendix. We can summarize the theoretical energy spectrum of the toroidal ^{12}C nucleus in Table VI and in Fig. 2.

TABLE VI. The theoretical spectrum of ^{12}C in a toroidal configuration. Here, $E_x = E_I - E_0$, E_I is the energy of a state in the multiplet, E_0 is the toroidal ground state energy, $\epsilon_0 = 1.25$ MeV by matching with the experimental spectrum, and N is the number of doubly-degenerate states in the multiplet.

Ground State & Multiplets	$\frac{E_x}{\epsilon_0}$	E_I (MeV)	$I_z = I$ states	N
Toroidal Ground State	0	7.654	0^+	1
$[(1p1h)_{12}]^-$	3	11.41	$0^-, 2(1^-), 2(2^-), 2(3^-), 4^-$	8
$[(1p1h)_{02}]^+$	4	12.66	$1^+, 2(2^+), 3^+$	4
$[(2p2h)_{12}]^+$	6	15.16	$3(0^+), 5(1^+), 4(2^+), 2(3^+), 2(4^+), 5^+, 6^+$	18
$[(1p1h)_{12\nu}(1p1h)_{12p}]^+$	6	15.16	$15(0^+), 27(1^+), 25(2^+), 20(3^+), 16(4^+), 12(5^+), 8(6^+), 4(7^+), 8^+$	128
$[(1p1h)_{12}(1p1h)_{02}]^-$	7	16.42	$4(0^-), 7(1^-), 5(2^-), 3(3^-), 2(4^-), 2(5^-), 6^-$	24
$[(1p1h)_{12\nu}(1p1h)_{02p}]^-$	7	16.42	$8(0^-), 15(1^-), 12(2^-), 9(3^-), 8(4^-), 7(5^-), 4(6^-), 7^-$	64
$[(1p1h)_{13}]^+$	8	17.67	$1^+, 2(2^+), 2(3^+), 2(4^+), 5^+$	8
$[(2p2h)_{02}]^+$	8	17.67	$0^+, 1^+, 4^+$	3
$[(1p1h)_{02\nu}(1p1h)_{02p}]^+$	8	17.67	$6(0^+), 8(1^+), 3(2^+), 4(3^+), 6(4^+), 4(5^+), 6^+$	32
$[(1p1h)_{03}]^-$	9	18.92	$2^-, 2(3^-), 4^-$	8
$[(3p3h)_{12}]^-$	9	18.92	$0^-, 2(1^-), 2(2^-), 2(3^-), 4^-$	8
$[(2p2h)_{12\nu}(1p1h)_{12p}]^-$	9	18.92	$30(0^-), 59(1^-), 55(2^-), 47(3^-), 36(4^-), 25(5^-), 16(6^-), 10(7^-), 6(8^-), 3(9^-), 10^-$	288
$[(2p2h)_{12p}(1p1h)_{12\nu}]^-$	9	18.92	(same as above)	288
$[(2p2h)_{12}(1p1h)_{02}]^+$	10	20.15	$3(0^+), 6(1^+), 6(2^+), 5(3^+), 3(4^+), 5^+$	24
$[(2p2h)_{12p}(1p1h)_{02\nu}]^+$	10	20.15	$15(0^+), 30(1^+), 29(2^+), 25(3^+), 18(4^+), 11(5^+), 7(6^+), 5(7^+), 3(8^+), 9^+$	144
$[(2p2h)_{12\nu}(1p1h)_{02p}]^+$	10	20.15	(same as above)	144
$[(2p2h)_{02}(1p1h)_{12}]^-$	11	21.40	$4^-, 2(3^-), 2(2^-), 2(1^-), 0^-$	8
$[(4p4h)_{12}]^+$	12	22.65	0^+	1
$[(2p2h)_{12\nu}(2p2h)_{12p}]^+$	12	22.65	$69(0^+), 130(1^+), 117(2^+), 96(3^+), 78(4^+), 58(5^+), 42(6^+), 26(7^+), 16(8^+), 8(9^+), 5(10^+), 2(11^+), 12^+$	628
$[(3p3h)_{12}(1p1h)_{02}]^-$	13	23.90	$0^-, 2(1^-), 2^-$	4
$[(3p3h)_{12\nu}(1p1h)_{02p}]^-$	13	23.90	$8(0^-), 15(1^-), 12(2^-), 9(3^-), 8(4^-), 7(5^-), 4(6^-), 7^-$	64
$[(3p3h)_{12p}(1p1h)_{02\nu}]^-$	13	23.90	(same as above)	64
$[(2p2h)_{12}(2p2h)_{02}]^+$	14	25.15	$0^+, 1^+, 2^+$	3
$[(2p2h)_{12\nu}(2p2h)_{02p}]^+$	14	25.15	$13(0^+), 23(1^+), 20(2^+), 15(3^+), 13(4^+), 10(5^+), 7(6^+), 3(7^+), 2(8^+), 9^+, 10^+$	108

For simplicity, we have represented the single-particle potential of a toroidal nucleus by a simple harmonic oscillator potential, Eq. (1). Such a representation is adequate for the lowest few toroidal shells. However, in a more realistic case, the single-particle potential should follow the toroidal density and should be a diffused potential with a finite depth. The higher toroidal shells are

expected to be unbound. As a consequence, there will be a termination of the (nph) toroidal excitations, indicated by the absence of toroidal particle-hole excitations at high energies and a rapid decrease of the density of toroidal particle-hole excitation states. It will be of interest to search for the excitation energy maximum in ^{12}C at which the toroidal particle-hole excitation states ceases to appear.

V. EXPLORATORY COMPARISON OF THEORETICAL TOROIDAL ^{12}C STATES WITH EXPERIMENTAL SPECTRUM

In the last few sections, we show that the ^{12}C nucleus in a toroidal configuration possess a distinct spectrum of states with a well defined pattern of spins, parities, and excitation energies. They arise from particle-hole excitations from one toroidal shell to another toroidal shell and can be conveniently called “toroidal states”. The spectrum constitutes the signature of the ^{12}C nucleus in the toroidal configuration. Using such a signature, we would like to explore whether there may be toroidal states in ^{12}C with the 0^+ Hoyle state at 7.654 MeV as the ground state of the toroidal band.

In our exploratory survey, we expect that if it co-exists with the oblate spheroidal ground state, the toroidal ground state of ^{12}C and the low-lying toroidal multiplets will show up as ^{12}C resonances with a large probability to breakup into 3 alpha particles, because the triangular clusters of three alpha particles has a large overlap with the configuration of a toroidal nucleus. Accordingly, we search for good candidate states in $^{10}\text{B}(^3\text{He}, p)^{12}\text{C}^* \rightarrow 3\alpha$ and $^{11}\text{B}(^3\text{He}, d)^{12}\text{C}^* \rightarrow 3\alpha$ reactions [14–16] as shown in Figs. 3, 4, and 5. We shall discuss the results of our search in the following subsections.

A. Search for toroidal states with the $^{11}\text{B}(^3\text{He}, d)^{12}\text{C}^* \rightarrow 3\alpha$ reaction

In the experiments of Kirsebom *et al.* [14, 15], excited intermediate $^{12}\text{C}^*$ states were produced by the bombardment of the ^3He projectile at 8.5 MeV onto a ^{11}B target in the reaction $^3\text{He} + ^{11}\text{B} \rightarrow d + ^{12}\text{C}^*$, with the subsequent breakup of the $^{12}\text{C}^*$ intermediate state into three alpha particles, $^{12}\text{C}^* \rightarrow 3\alpha$. The complete kinematic data of the final deuterium d and the 3 alpha particles have been recorded with detectors of fine resolutions and segmentation. The complete kinematics data allow the determination of the energy of the intermediate $^{12}\text{C}^*$ state, the history of its subsequent decay, whether through the 0^+ or the 2^+ state of ^8Be , and the energy distribution Dalitz plot of the 3 alpha particles. From these pieces of information, the spins and parities of the prominent ^{12}C resonances can be inferred. The complete kinematic data allows the removal of most of the random coincidences and decay channels that do not involve the production

in linear scale. Figs. 3(b) and 4(b) give the energy levels from the experimentally identified ^{12}C excited states from the compilation of [13]. The excitation energy E relative to the energy of ^{12}C ground state is given on the left axis.

The experimental excitation functions in Figs. 3(a) and 4(a) indicate that the 0^+ Hoyle state at $E=7.654$ MeV is prominently excited, as are the 3^- state at 9.654 MeV, the 1^- state at 10.847 MeV, the 2^- state at 11.837 MeV, the 4^- state at 13.314 MeV, and the 1^+ state at 12.71 MeV.

The theoretical toroidal states energy levels are presented in Figs. 3(c) and 4(c). In the large radius approximation with the neglect of the small spin-orbit and residual interactions, the gross pattern of the toroidal states depends only on a single parameter, the major radius R . The simplified theoretical spectrum indicates that the lowest excited states are the $[(1p1h)_{12}]^-$ multiplet of $\{4^-, 2(3^-), 2(2^-), 2(1^-), 0^-\}$ at $E_x = 3\epsilon_0 = 3\hbar^2/2mR^2$, and another $[(1p1h)_{02}]^+$ multiplet of $\{1^+, 2(2^+), 3^+\}$ at $E_x = 4\epsilon_0$, as given in Table VI and Fig. 2, 3(c), and 4(c). The degeneracy within the multiplet arises from the neglect of spin-orbit splitting and residual interactions.

By comparison of the experimental and the theoretical spectrum, we find that the lowest theoretical multiplet in toroidal ^{12}C contains states with spins and parities that coincide with those of the experimental states. It is therefore reasonable to identify the 0^+ Hoyle state at 7.654 MeV to be the $(0p0h)$ ground state of the toroidal configuration and the set of lowest $\{3^-(9.654 \text{ MeV}), 1^-(10.847 \text{ MeV}), 2^-(11.837 \text{ MeV}), 4^-(13.314 \text{ MeV})\}$ states to be members of the $(1p1h)_{12}^-$ multiplet.

We get additional support to identify these four states as members of a multiplet from the strengths of the excitation function. Upon treating the stripping reaction $^{11}\text{B}(^3\text{He}, d)^{12}\text{C}^*$ leading to toroidal particle-hole states in $^{12}\text{C}^*$ as a two step process, the probability amplitude is the product of the amplitude (i) for the stripped proton to excite and to combine with the ^{11}B system to come to the toroidal doubly-close shell of $^{12}\text{C}^*$, and the amplitude (ii) for the particle-hole excitation from the close shell to the toroidal (one particle)-(one hole) excitation. The amplitude (i) is independent of the members of the multiplet, and the latter amplitude (ii) depends only on the degree of fullness of the closed occupied $\Lambda_z = 1$ (or 0) shell and the degree of emptiness of the unoccupied $\Lambda_z = 2$ shell, which are the same for all members of the shell-to-shell particle-hole multiplet. Consequently, all members of the $(1p1h)_{12}^-$ multiplet should be approximately equally produced. An examination of the widths and heights of the identified lowest $\{3^-, 1^-, 2^-, 4^-\}$ states indicate that these four are approximately equally populated, supporting their identification as members of the $(1p1h)_{12}^-$ multiplet.

Following such an identification, we set the average excitation energy of the four states $\{3^-, 1^-, 2^-, 4^-\}$ at 11.41 MeV to be the excitation energy of the $(1p1h)_{12}^-$ multiplet. Such a matching leads to the theoretical en-

ergy scale,

$$\epsilon_0 = 1.25 \text{ MeV}. \quad (19)$$

By the definition of ϵ_0 as $\hbar^2/2mR^2$, we obtain the corresponding equilibrium major radius,

$$R = 4.06 \text{ fm}. \quad (20)$$

The knowledge of ϵ_0 allows the determination of the theoretical toroidal spectrum of ^{12}C as tabulated in Table VI and shown in Figs. 2-5. In particular, we find that the 1^+ state at $E_z=12.710$ MeV approximately matches the 1^+ state in the multiplet of $(1p1h)_{02}^+$. The 1^+ state at $E_z=15.111$ MeV approximately matches the 1^+ state in the multiplet of $(2p2h)_{12}^-$. There also appears to be a hint of an alternating change of parity of the states, similar to the alternating parity of the theoretical levels. However, whether such coincidental comparison can remain in the presence of residual interactions remains to be investigated.

The excited states of ^{12}C contains a 4^+ state at 13.3 MeV [70] and another 4^+ state at 14.079 MeV [13]. The sequence of the Hoyle state $0_2^+(7.654 \text{ MeV})$, $2_2^+(9.870 \text{ MeV})$, and either one of the two 4^+ states follow approximately the relation between the angular momentum and the rotational energy of a rotor. From the analysis of the interacting cluster model, it is found that the sequence of the 0_1^+ (ground state), $2_1^+(4.33 \text{ MeV})$, and $4_2^+(14.079 \text{ MeV})$ form the rotational states of the ground band, whereas the sequence of the Hoyle state $0_2^+(7.654 \text{ MeV})$, $2_2^+(9.870 \text{ MeV})$, and $(4_1^+)(13.3 \text{ MeV})$ state [70] form a rotational band with a different moment of inertia [71]. The presence of a rotational band built on the Hoyle state is consistent with the identification of the Hoyle state as the head of the toroidal multiplet suggested by particle-hole excitation data from the stripping reaction we have presented here. In contrast to the Hoyle state and the $(1p1h)$ states, the stripping reaction $(^3\text{He}, d)$ does not prominently excite the $2^+(9.870 \text{ MeV})$, and $4^+(13.3 \text{ MeV})$ states of the rotational band of the Hoyle state because they are probably collective states in nature.

While the above comparison indicates that the Hoyle state and many of its higher excited states may be tentatively attributed to the ^{12}C nucleus in a toroidal configuration, further confirmation and careful examination are necessary. There appear to be many more theoretical states compared to the experimentally identified states. The large number of theoretical states means that further experimental works are needed. The experimental search for these states may be difficult as they may be so broad that they may be hidden under the resonances of the other observed and identified states. Theoretically, refinement of the theoretical work using toroidal basis to include spin-orbit and residual interactions will determine more precisely the locations of these states so to ascertain better whether such a toroidal description has approximate validity.

With regard to the question of uncovering the remaining members of the multiplets, it is interesting to note

the remarkable recent advances in employing complete kinematics to study the breakup of ^{12}C resonances into three α particles in Ref. [14]. The measurement of [14] is essentially free of background [66]. Interesting enough, as noted in [14], the strength of the excitation function away from the clean peaks of these states in Fig. 3(a) indicate that additional overlapping resonances of ^{12}C may have been produced in the process. They constitute non-vanishing strengths in the Dalitz plot and may represent the un-identified members of the toroidal multiplet. Thus, the search and identify these missing members of the $[(1p1h)_{12}^-]$ and $(1p1h)_{02}^+$ multiplets from the underlying strengths of the excitation function in Fig. 3 may provide a test of the toroidal description of the ^{12}C states. In this regard, the technique of identifying resonances by the patterns in the Dalitz plot [69] may find its useful application in the determination of the spin and parity of the states in the underlying structure.

We can seek additional support for the toroidal multiplet description of the ^{12}C states. We focus our attention on the excitation function in the excitation energy range $9 \leq E \leq 14.5$ MeV in Fig. 4(a), where the 1^- , 2^- , and 4^- resonances are well separated and identified. However, in the same excitation energy range in Fig. 4(a), there appears an underlying broad structure beneath the peaks of the identified resonances. We take the view that by nature of the background-free measurement with full kinematics in the determination of the spectrum of Fig. 4(a), the board structure likely originates from the remaining members of the toroidal multiplets that are also produced with each state approximately in equal strength in the stripping $^{11}\text{B}(^3\text{He},d)^{12}\text{C}^* \rightarrow 3\alpha$ reaction.

It is illuminating to estimate the number of the produced but un-identified $^{12}\text{C}^*$ resonances in the underlying broad structure in the range of excitation energies in Fig. 4(a) by using the excitation function strengths of the resolved resonances in the range as a yard stick. In the data of Fig. 4(a), the 1^- (10.847 MeV), 2^- (11.837 MeV), and 4^- (13.314 MeV) resonances are members of the multiplet arising from single-particle excitations populating a one-particle-one-hole state in the $\Lambda_z=2$ shell. The strengths of each the three peaks defines roughly a definite measure which we call “single-particle unit”, with approximately the same area for each of the three peaks, and each single-particle unit leads to the production of one $^{12}\text{C}^*$ state. On that basis of using that (average) area as a yardstick, we find that in the energy range of Fig. 4(a) up to the instrumental cut-off excitation energy of ~ 14.5 MeV, there are approximately 3 to 5 units of single-particle strength for natural parity states and 2 to 4 units for the un-natural parity states in the underlying overlapping resonances, with a considerable degrees of uncertainty in these numbers due to the uncertainty in separating out the resolved peaks from the underlying broad structure. It is gratifying that the numbers of remaining un-identified members in the multiplet fall within the range of numbers of states estimated to be present in the underlying broad structure in Fig. 4(a).

By this comparison, it appears that the total number of identified and unidentified resonances produced in the $^{11}\text{B}(^3\text{He},d)^{12}\text{C}^* \rightarrow 3\alpha$ reaction matches approximately the total number of states of the $(1p1h)_{12}^-$ and $(1p1h)_{02}^+$ multiplets, providing an additional support for the tentative toroidal multiplet description of these states in ^{12}C .

B. Toroidal states production in the $^{10}\text{B}(^3\text{He},p)^{12}\text{C}^*$ reaction

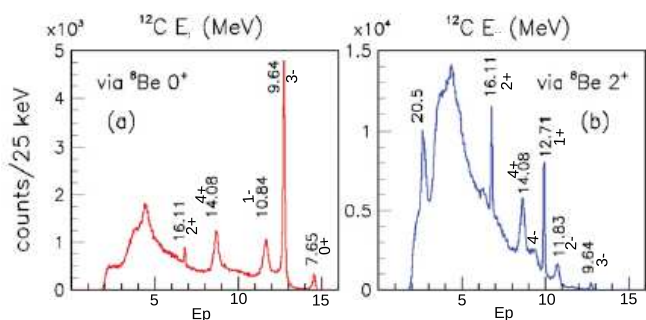


FIG. 5. (Colour online.) Experimental excitation functions of the reaction $^{10}\text{B}(^3\text{He},p)^{12}\text{C}^* \rightarrow 3\alpha$ as a function of the proton energy E_p from Alcorta *et al.*[16]. The decay of $^{12}\text{C}^*$ goes through the 0^+ state of ^8Be in (a) and through the 2^+ state of ^8Be in (b). The excitation energies, spins, and parities of identified resonances of $^{12}\text{C}^*$ are indicated. Please note the different count scales on the y-axes in Figs. (a) and (b).

In the experiment to use the $^{10}\text{B}(^3\text{He},p)^{12}\text{C} \rightarrow 3\alpha$ reaction to study the excited states of ^{12}C by Alcorta *et al.*[16], the ^3He projectile collides with a ^{10}B target nucleus at a beam energy of 4.9 MeV to produce a proton and 3 alpha particles. The complete kinematics data of all four final particles were collected using detectors of fine resolution and segmentation. Again, the full knowledge of the complete kinematics provides information on the energy of the intermediate $^{12}\text{C}^*$ state, the history of its decay through ^8B , and the three alpha particle Dalitz plots to facilitate the assignment of spins and parities. Contributions from direct reactions leading to the production of intermediate states other than $^{12}\text{C}^*$ have been eliminated as much as possible. The excitation function of the 3α spectrum can be considered to be essentially free of background, pending future removal of the small $^3\text{He}+^{10}\text{B} \rightarrow ^8\text{Be}+^5\text{Li} \rightarrow ^8p+\alpha+^5\text{Li}$ and $^3\text{He}+^{10}\text{B} \rightarrow \alpha+^9\text{B} \rightarrow \alpha+\alpha+^5\text{Li}$ contributions [66].

The $(^3\text{He},p)$ reaction strips a neutron and a proton from the ^3He projectile and deposits them onto the ^{10}B target. The selection of the final state of three alpha particles and a scattered proton allow one to judiciously examine those events in which the stripped pair of nucleons interact with the ^{10}B system to re-arrange themselves

into a toroidal configuration with a subsequent decay into three alpha particles. At the energy appropriate for the production of the toroidal ground state, the stripped neutron and proton can excite the nucleons in ^{10}B to rearranged themselves into a toroidal configuration leaving two holes at the top of the fermi surface. Filling the two holes with the stripped nucleons in the closed toroidal shell will lead to the production of the (0p0h) toroidal ground state. Filling one hole in the $\Lambda_z=1$ shell and another unoccupied state by the stripped nucleons in the $\Lambda_z=2$ shell at another appropriate excitation energy will lead to a (1p1h) toroidal state in $^{12}\text{C}^*$, and filling up two empty states in the $\Lambda_z=2$ shell will lead to a (2p2h) toroidal state at a still higher excitation energy. The $^{10}\text{B}(^3\text{He},p)3\alpha$ reaction should favorably populate the (0p0h), (1p1h), and (2p2h) toroidal excitations of $^{12}\text{C}^*$ at different excitation energies.

Experiment data $^{10}\text{B}(^3\text{He},p)^{12}\text{C} \rightarrow 3\alpha$ reaction [16] as shown in Fig. 5 in the three alpha breakup indicate that the Hoyle state, the lowest $\{1^-, 2^-, 3^-, 4^-\}$ and 1^+ states are prominently produced, lending additional support to the description that the Hoyle state may be tentatively identified as the toroidal ground state, the $\{1^-, 2^-, 3^-, 4^-\}$ as members of the toroidal (1p1h)₁₂ multiplet, and the $1^+(12.71 \text{ MeV})$ state to be a member of the (1p1h)₀₂ multiplet. The possibility of the (2p2h) excitations in the $^{10}\text{B}(^3\text{He},p)^{12}\text{C}^*$ reaction lead to an enhanced excitation function at higher excitation energies. It is interesting to note that the experimental $4^+(14.08 \text{ MeV})$ state and the $2^+(16.11 \text{ MeV})$ falls in the vicinity of the theoretical (2p2h)₁₂⁺ multiplet whose members include a 2^+ and a 4^+ state. Whether these two states can be identified as two members of the (2p2h)₁₂⁺ multiplet will require further theoretical and experimental investigations.

In Fig. 5 the produced resolved states appear as sharp peaks on top of an underlying broad structure. If we employ the earlier method using the areas of the excitation function covered by known resonances as a ‘single-particle’ yard stick to estimate the number of states involved in the underlying broad structure, we would come up with the result that the number of states comprising the underlying broad structure in Fig. 5 is an order of magnitude greater than number of resolved and identified resonances. Thus in addition to the production of the resolved and identified states that have been mentioned as possible members of the toroidal multiplets, the underlying structure represents also possible produced members of the toroidal multiplets in the $^{10}\text{B}(^3\text{He},p)^{12}\text{C}^* \rightarrow 3\alpha$ reaction of Ref. [16]. They have the same property of decaying into three alpha particles, they are in the same energy region as the resolved members of the multiplet, and all these state in the multiplet may share similar shell-to-shell excitation probability amplitudes.

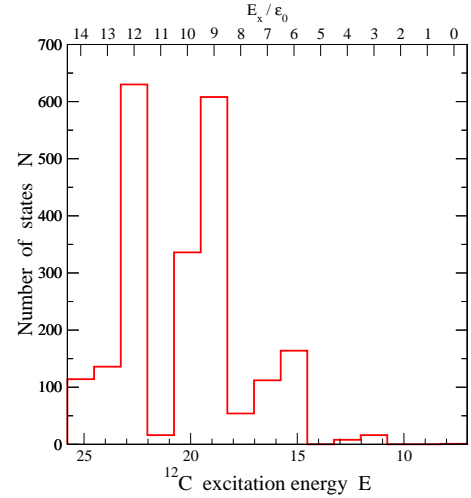


FIG. 6. (Colour online.) Number of toroidal states as a function of the excitation energy E relative to the ground state for the ^{12}C nucleus in a toroidal configuration.

The experimental excitation function in Fig. 5 provides valuable information on the variation of the the number of excited $^{12}\text{C}^*$ states as a function of excitation energy. The excitation functions rise up as a function of increasing excitation energy E , starting at around $E \sim 12$ -14 MeV, reaching a maximum at around $E \sim 18.5$ MeV, and decrease rapidly at around $E \sim 22$ MeV. Theoretically in the toroidal model of $^{12}\text{C}^*$, there is an increase in numbers of toroidal states with increasing excitation energy as shown in Table VI and plotted in Fig. 6. It rises up around $E \sim 14.5$ MeV and has two peaks structure with fine details at 19 and 23 MeV. It decreases rapidly for E_x greater than ~ 22 MeV. The inclusion of the spin-orbit and residual interactions as well as the large width of these toroidal states will smear the theoretical peaks, but the general structure of a peak around the excitation region of $E \sim 18$ MeV mimicks qualitatively the shape of the experimental excitation function in Fig. 5. It will be of interest to investigate whether such a correlation with the shape of the experimental excitation function may indeed corresponds to the theoretical variation of the density of toroidal states. It will also be of interest to find out whether there is also the termination of the toroidal particle-hole excitation multiplets at high excitation energies, when the unoccupied single-particle states at the higher shells become unbound.

In addition to the experimental results discussed in this section, many recent experiments have been carried out to study the Hoyle state and the higher excited states. Whelen *et al.* use the $^{12}\text{C}(^3\text{He},^3\text{He})^{12}\text{C}^* \rightarrow 3\alpha$ reaction [7] at a beam energy of $E(^3\text{He})=46$ MeV. Barbui *et al.* [17] studied 3 alpha particles in coincidence in forward angles using the inverse kinematic reaction $^{20}\text{Ne} + \alpha \rightarrow 3\alpha + X$ with ^{20}Ne on a gaseous ^4He target at a maximum beam energy of 12 MeV/nucleon. These measurements uncover many relatively narrow resonances in $^{12}\text{C}^*$ at high excitation energies in conjunction with the Hoyle state at

7.654 MeV. Many of the resonances at very high energies have not been completely identified and analyzed to gain information on their spins and the parities. Further future analysis of the quantum numbers and the nature of these many resonances will enhance our knowledge of the excited states of the ^{12}C nucleus and will provide a test of different models.

VI. TOROIDAL ^{12}C IN TOROIDAL CONSTRAINT DYNAMICS

Our exploratory investigation points to the need to devise tools within the mean-field theory that can constrain the ^{12}C nucleus so to possess local toroidal energy equilibrium configurations. As the ground state of ^{12}C has the topology of an oblate spheroid, we should be prepared to examine the toroidal configuration as excited diabatic states of the system. Success for formulating such tools will be useful not only for the ^{12}C nucleus but also for the many diabatic states that may be associated with the large region of toroidal high-spin isomers in α -conjugate nuclei up to $A \sim 70$ [56–58]. It will also be useful for the investigation of diabatic toroidal states in the intermediate and superheavy mass region for which some recent progress has been made [60, 67, 68].

We consider a Hamiltonian H_0 which contains already many constraints that have been imposed on the system. We wish to impose an additional toroidal constraint to hold the nucleus in a toroidal shape. For this purpose, we introduce a radial moment d_0^2 to characterize the radial property of the density distribution that can constrain the density into a toroidal shape,

$$d_0^2 = \left\{ \int d\mathbf{r} D(\mathbf{r})(\rho - \langle \hat{\rho} \rangle)^2 \right\}, \quad (21)$$

where $\langle \hat{\rho} \rangle$ is the expectation value of the coordinate $\hat{\rho} = \rho = \sqrt{x^2 + y^2}$,

$$\langle \hat{\rho} \rangle = \int d\mathbf{r} \sum_{i=1}^A \psi_i^*(\mathbf{r}) \hat{\rho} \psi_i(\mathbf{r}), \quad (22)$$

and $D(\rho, z)$ is the nuclear density which can be determined self-consistently from the set of the wave functions $\{\psi_i\}$ of occupied states

$$D(\mathbf{r}) = \sum_{i=1}^A \psi_i^*(\mathbf{r}) \psi_i(\mathbf{r}). \quad (23)$$

The constraint of a fixed toroidal radial moment d_0^2 , can be imposed with the additional Lagrange multiplier λ ,

$$H = H_0 + \lambda \left\{ \int d\mathbf{r} D(\mathbf{r}) (\rho - \langle \hat{\rho} \rangle)^2 - d_0^2 \right\} \quad (24)$$

Upon a minimization of the Hamiltonian H with respect to a variation in ψ_i^* , we have

$$\frac{\delta H}{\delta \psi_i^*} = \frac{\delta H_0}{\delta \psi_i^*} + \lambda \int d\mathbf{r} (\rho - \langle \hat{\rho} \rangle)^2 \psi_i$$

$$+ (\text{terms involving } \frac{\delta \langle \hat{\rho} \rangle}{\delta \psi_i^*}) \quad (25)$$

To the extent that the change of the bulk $\langle \hat{\rho} \rangle$ with respect to the change of individual single-particle states ψ_i^* is small when the occupation numbers of the states have settled down and do not change, the last term of the above variation can be neglected. Writing H_0 in terms of the single-particle Hamiltonian h_0 as

$$H_0 = \int d\mathbf{r} \sum_{i=1}^A \psi_i^*(\mathbf{r}) h_0 \psi(\mathbf{r}), \quad (26)$$

and we have

$$\frac{\delta H_0}{\delta \psi_i^*} = \int d\mathbf{r} h_0 \psi_i. \quad (27)$$

Under the toroidal constraint of Eq. (24), the minimization of H with respect to ψ_i^* leads to the single-particle Hamiltonian under the toroidal constraint

$$h' = h_0 + \lambda (\rho - \langle \hat{\rho} \rangle)^2. \quad (28)$$

In the case with a large R/d ratio, $\langle \hat{\rho} \rangle \sim R$. Thus, we observe that the last term of Eq. (28) is approximately in the same form as the toroidal potential of Eq. (1), with the Lagrange multiplier λ playing the role of the harmonic oscillator frequency ω_\perp^2 multiplied by the nucleon mass m . We obtain the result that with the addition of the toroidal constraint Eq. (21), the variation principle lead to a single-particle toroidal potential that is similar to the potential of Eq. (1) with the ω_\perp appearing as a variational parameter. For a given quadrupole moment that leads to the proper R , the variation λ will lead to the proper radial width d of the transverse degree of freedom.

Another approach to examine toroidal nuclei can be carried out in diabatic mean-field calculations [53]. This is achieved by constraining the occupation of the single-particle states so that at the locations of the crossing of two single-particle states at the top of the fermi surface, one does not choose to occupy the state of the lowest energy. Instead, one maintains the diabatic configuration with the occupation of the state with the highest overlap with the earlier state before the level crossing, leading to a diabatic energy equilibrium as in [53]. Diabatic calculations have been performed successfully for ^{24}Mg [53] and ^{28}Si [51]. It will be of interest to see whether diabatic calculations for ^{12}C will reveal the toroidal ^{12}C states as discussed here.

VII. CONCLUSIONS AND DISCUSSIONS

In spite of many investigations on the excited states of ^{12}C , the intrinsic structure of many excited states of ^{12}C nucleus remains an unresolved problem [32]. We explore a novel description for some excited states of ^{12}C for the reason that the ^{12}C nucleus, with 6 neutrons 6 protons, is a doubly-magic closed-shell nucleus in a toroidal potential. The strong shell effects associated with a toroidal

shape may allow a toroidal ^{12}C nucleus to co-exist with the ground state oblate spheroid. A dynamical generalization of the motion of the exchange nucleons between the clusters in Wheeler's classical model of ^{12}C as three α clusters will also generate a toroidal density if the nucleons exchanged between the clusters are allowed to circulate continuously from cluster to cluster. The toroidal description of ^{12}C is therefore a dynamical derivative of Wheeler's triangular cluster model. Furthermore, the importance of the toroidal shell structure has recently been highlighted by possible populations of toroidal high-spin isomers as was predicted by a number of theoretical investigations [51]. Many excited states of ^{12}C also decays predominantly into three alpha particles which have a large overlap with a toroidal configuration.

Nucleons in a toroidal potential will generate single-particle states obeying the proper shell structure appropriate for such a peculiar density. Consequently the toroidal shell structure gives rise to a set of excited states bearing the imprint of the intrinsic properties of the toroidal nucleus. Specifically, the clustering of the single-particle state energy levels into shells lead to the classification of toroidal Λ_z shells, which show up as different particle-hole excitations from one toroidal shell to another. The spectrum of a toroidal nucleus is characterized by these multiple shell-to-shell step-wise excitation multiplets of various spin, parities, and excitation energies.

We have obtained the theoretical signature of the ^{12}C nucleus in the toroidal configurations and have confronted the data with theory. We find that the Hoyle state may be tentatively attributed to be the ground states of a ^{12}C nucleus in the toroidal configuration and the lowest excited states of $3^-, 1^-, 2^-$ and 4^- may be members of the $(1p1h)_{\bar{1}2}$ multiplet and the $1^+(12.71 \text{ MeV})$ state may be members of the $(1p1h)_{\bar{0}2}$ multiplet. The sequence of the Hoyle state, the 2^+ state, and 4^+ state may be the rotational band of the Hoyle state. There is a hint that parity of the states appear to be approximately alternating, in a way similar to the prediction of the theory.

In spite of the tentatively encouraging results, the evidence is not yet completely conclusive as the complete set of multiplets have not been found. There are many more states in the theoretical toroidal description, as compared to the identified resonances. Experimentally, the search for the remainder states in the multiplet will be needed. The presence of prominent underlying broad structures in the excitation functions of the $^{11}\text{B}(^3\text{He}, d)^{12}\text{C} \rightarrow 3\alpha$ reaction of Ref. [14] indicates that the remainder members of the produced multiplet may be contained in the underlying broad structures. Experimental data from the $^{10}\text{B}(^3\text{He}, p)^{12}\text{C} \rightarrow 3\alpha$ reaction in [16] provide additional support for the possible toroidal description of the Hoyle state and the low-lying excited states. Furthermore, the $^{10}\text{B}(^3\text{He}, p)^{12}\text{C} \rightarrow 3\alpha$ data at higher energies suggests possible copious production of toroidal states which appear as a large underlying broad structure underneath the

resolved resonances. Theoretical predictions and their comparisons with the experimental data therefore suggest that there may be a large number of toroidal $^{12}\text{C}^*$ states over a large energy region that readily breakup into three alpha particles, which may have implications in energy-producing mechanisms.

In future theoretical work, it is necessary to include spin-orbit and residual interactions so as to define better the splitting of the multiplets and to guide where these states may be more precisely located. The knowledge of a better wave function will allow the evaluation of the toroidal moment of inertia of the Hoyle state, for comparison with the observed moment of inertia. Theoretical mean-field calculations with a toroidal constraint will need to be carried out to show whether there are adiabatic toroidal ^{12}C states that can co-exist with the ground oblate spheroid state.

Acknowledgments

The research was supported in part by the Division of Nuclear Physics, U.S. Department of Energy under Contract DE-AC05-00OR22725.

Appendix A: (nph) multiplets of states of toroidal ^{12}C at higher excitation energies

1. $[(1p1h)_{12}(1p-1h)_{02}]^-$ multiplet at $E_x=7\epsilon_0$ involving two identical nucleons

We like to examine the I_z states of $[(1p1h)_{12}(1p-1h)_{02}]^-$ at $E_x=\Delta E_{12} + \Delta E_{02}=7\epsilon_0$ involving identical particles with $(|\Lambda_z|=1) \rightarrow (|\Lambda_z|=2)$ and $(|\Lambda_z|=0) \rightarrow (|\Lambda_z|=2)$ excitations. Because the particle states in the $|\Lambda_z|=2$ shell of identical particles must obey the Pauli Principle, we need to combine the particle pair first before we combine them with the hole pairs.

The pair of particles in the $\Lambda_z=2$ shell combine as in the following Table VII below

TABLE VII. Combination of two particles states in $|2 \pm 5/2\rangle$ and $|2 \pm 3/2\rangle$ orbitals in the $\Lambda_z=2$ shell

two particle configuration	I_z^π
$\{[2(5/2)][2(3/2)]\}$	4^+
$\{[2(5/2)][2(-3/2)]\}$	1^+
$\{[2(3/2)][2(-3/2)]\}$	0^+
$\{[2(-5/2)][2(5/2)]\}$	0^+
$\{[2(-5/2)][2(3/2)]\}$	$(-1)^+$
$\{[2(-5/2)][2(-3/2)]\}$	$(-4)^+$

So the pair of (2p) in the $\Lambda_z=2$ shell combine to be $\{4^-, 1^+, 0^+, 0^+, (-1)^+, (-4)^+\}$. It suffices to consider only $4^+, 1^+$ and 0^+ and get the other possibility by reversing the sign. Now combine with the hole states $|0 \pm 1/2\rangle$ with $\{|1 \pm 3/2\rangle$ and $|1 \pm 1/2\rangle$, we get

TABLE VIII. Combination of two holes states in of (i) $|0 \pm 1/2\rangle$ with (ii) $|1 \pm 3/2\rangle$ and $|1 \pm 1/2\rangle$ orbitals in the $\Lambda_z=2$ shell

hole in $ 0 \pm 1/2\rangle$ State	hole in $ 1 \pm 3/2\rangle$ and $ 1 \pm 1/2\rangle$			
	$3/2^-$	$1/2^-$	$(-1/2)^-$	$(-3/2)^-$
$1/2^+$	2^-	1^-	0^-	$(-1)^-$
$-1/2^+$	1^-	0^-	$(-1)^-$	$(-2)^-$

TABLE IX. The I_z^π states of the $[(1p1h)_{12}(1p1h)_{02}]^-$ multiplet at $E_x = 7\epsilon_0$.

2 hole in $\Lambda_z = 0$ and $\Lambda_z = 1$ shell	2 particles in $\Lambda_z = 2$ shell		
	4^+	1^+	0^+
2^-	2^-	$(-1)^-$	$(-2)^-$
1^-	3^-	0^-	$(-1)^-$
0^-	4^-	1^-	0^-
$(-1)^-$	5^-	2^-	1^-
1^-	3^-	0^-	$(-1)^-$
0^-	4^-	1^-	0^-
$(-1)^-$	5^-	2^-	1^-
$(-2)^-$	6^-	3^-	2^-

We find that the $[(1p1h)_{12}(1p1h)_{02}]^-$ multiplet at $E_x = 7\epsilon_0$ contains 24 doubly-degenerate negative-parity states: $\{6^-, 2(5^-), 2(4^-), 3(3^-), 5(2^-), 7(1^-), 4(0^-)\}$.

2. $[(1p1h)_{12\nu}(1p-1h)_{02p}]^-$ multiplet at $E_x=7\epsilon_0$ involving a neutron and a proton

We have considered the $(2p2h)$ excitations involving only one type of nucleons which obey the Pauli principle. We consider here $(2p-2h)$ excitations involving neutrons and protons by combining the neutron and proton $(1p-1h)$ excitations independently. The $[(1p1h)_{12\nu}(1p-1h)_{02p}]^-$ at $E_x=7\epsilon_0$ excites a neutron from the $\Lambda_z=1$ shell and a proton from the $\Lambda_z=0$ shell to the $\Lambda_z=2$ shell. The spins and parities of the $[(1p1h)_{12\nu}(1p-1h)_{02p}]^-$ multiplet

are given in Table X.

TABLE X. The I_z^π states of the $[(1p1h)_{12\nu}(1p1h)_{02p}]^-$ toroidal multiplet at $E_x = 7\epsilon_0$ in ^{12}C for exciting a neutron and a proton from the $\Lambda_z=1$ shell and a proton from the $\Lambda_z=2$ shell to the $\Lambda_z=2$ shell.

$(1p1h)_{12\nu}$ State	$(1p1h)_{02p}$ State			
	3^+	2^+	2^+	1^+
4^-	7^-	6^-	6^-	5^-
3^-	6^-	5^-	5^-	4^-
2^-	5^-	4^-	4^-	3^-
1^-	4^-	3^-	3^-	2^-
3^-	6^-	5^-	5^-	4^-
2^-	5^-	4^-	4^-	3^-
1^-	4^-	3^-	3^-	2^-
0^-	3^-	2^-	2^-	1^-
$(-4)^-$	$(-1)^-$	$(-2)^-$	$(-2)^-$	$(-3)^-$
$(-3)^-$	0^-	$(-1)^-$	$(-1)^-$	$(-2)^-$
$(-2)^-$	1^-	0^-	0^-	$(-1)^-$
$(-1)^-$	2^-	1^-	1^-	0^-
$(-3)^-$	0^-	$(-1)^-$	$(-1)^-$	$(-2)^-$
$(-2)^-$	1^-	0^-	0^-	$(-1)^-$
$(-1)^-$	2^-	1^-	1^-	0^-
0^-	3^-	2^-	2^-	1^-

This table show that the $[(1p1h)_{12\nu}(1p1h)_{02p}]^-$ multiplet contains a set of 64 states $\{7^-, 4(6^-), 7(5^-), 8(4^-), 8(3^-), 8(2^-), 8(1^-), 8(0^-), 7((-1)^-), 4((-2)^-), (-3)^-\}$. If we reverse the sign of the $(1p1h)_{02p}$ state, we get the same set of 64 states except that the signs of I_z is reversed if it is non-zero, and it has a different particle-hole combination if I_z is zero. So, upon combining these two sets, we find that the $[(1p1h)_{12\nu}(1p1h)_{02p}]^-$ multiplet contains a set of 64 doubly-degenerate states: $\{7^-, 4(6^-), 7(5^-), 8(4^-), 9(3^-), 12(2^-), 15(1^-), 8(0^-)\}$.

3. $(2p2h)_{02}^+$ multiplet at $E_x=8\epsilon_0$ involving two identical nucleons

To get the $(2p2h)_{02}^+$ excitations, it is simplest to combine the angular momentum of the two particles and the two holes separately before combining them together. For the two hole states, the $\{[0(-1/2)][0(1/2)]^{-1}\}$ form a closed shell, with a total $I_z = 0$. It is necessary only to consider the two particle states in $[2(\pm 5/2)][2(\pm 3/2)]$ for which results have already been obtained in Table III. We get the combination of $(2p2h)_{02}^+$ states as shown in Table XV.

TABLE XI. The I_z^π states of the $(2p2h)_{02}^+$ multiplet at $E_x = 2\Delta E_{02} = 8\epsilon_0$ for exciting two identical nucleons from the $\Lambda_z=0$ shell to the $\Lambda_z=2$ shell.

two holes	two particle configuration	I_z^π
$\{[0(1/2)][0(-1/2)]\}^{-1}$	$\{[2(5/2)][2(3/2)]\}$	4^+
	$\{[2(5/2)][2(-3/2)]\}$	1^+
	$\{[2(3/2)][2(-3/2)]\}$	0^+
	$\{[2(-5/2)][2(5/2)]\}$	0^+
	$\{[2(-5/2)][2(3/2)]\}$	$(-1)^+$
	$\{[2(-5/2)][2(-3/2)]\}$	$(-4)^+$

As one observes in Table XI, there are all together 3 doubly-degenerate (2 particle)-(2 hole) states, with $I_z^\pi = (\pm 4)^+, (\pm 1)^+$, and $(0^+)^2$ at an excitation energy $E_x = 2\Delta E_{02} \sim 8\epsilon_0$. So, the $(2p2h)_{02}^+$ multiplet consists of 3 doubly-degenerate states of $\{4^+, 1^+, 0^+\}$.

4. $[(1p1h)_{02\nu}(1p-1h)_{02p}]^+$ multiplet at $E_x=8\epsilon_0$ involving a neutron and a proton

We have considered the (2p2h) excitations involving only one type of nucleons. We can consider (2p-2h) excitations involving neutrons and protons by combining the neutron and proton (1p-1h) excitations independently.

TABLE XII. The I_z^π states of the $[(1p1h)_{02\nu}(1p1h)_{02p}]^+$ multiplet at $E_x=8\epsilon_0$

$(1p1h)_{02\nu}$ State	$(1p1h)_{02p}$ State			
	3^+	2^+	2^+	1^+
3^+	6^+	5^+	5^+	4^+
2^+	5^+	4^+	4^+	3^+
2^+	5^+	4^+	4^+	3^+
1^+	4^+	3^+	3^+	2^+
$(-3)^+$	0^+	$(-1)^+$	$(-1)^+$	$(-2)^+$
$(-2)^+$	1^+	0^+	0^+	$(-1)^+$
$(-2)^+$	1^+	0^+	0^+	$(-1)^+$
$(-1)^+$	2^+	1^+	1^+	0^+

Table XII contains the states $\{6^+, 4(5^+), 6(4^+), 4(3^+), 2(2^+), 4(1^+), 6(0^+), 4(-1)^+, 1(-2)^+\}$. Grouping the plus with the minus together, we find that the $[(1p1h)_{02\nu}(1p1h)_{02p}]^+$ multiplet at $E_x=8\epsilon_0$ contains the set of 32 doubly-degenerate states: $\{6^+, 4(5^+), 6(4^+), 4(3^+), 3(2^+), 8(1^+), 6(0^+)\}$.

5. $(3p3h)_{12}^-$ at $E_x=9\epsilon_0$ involving 3 identical particles

While the number of states in the (2 particle)-(2 hole) excitation in the $\Lambda_z=1$ state to the $\Lambda_z=2$ states are numerous in number, the number of state become fewer in

number for the (3 particle)-(3 hole) excitation because they approach the completion of a closed shell configuration with the excited single-particle $\Lambda_z = 2$ states.

TABLE XIII. The I_z^π states of the $(3p3h)_{12}^-$ multiplet excitations at $E_x = 9\epsilon_0$ involving three identical particles.

(3 particle)-(3 hole) configuration	I^π
$\{[1(3/2)][1(-1/2)][1(1/2)]\}^{-1} \{[2(-5/2)][2(-3/2)][2(3/2)]\}$	4^-
$\{[1(1/2)][1(-3/2)][1(3/2)]\}^{-1} \{[2(-5/2)][2(-3/2)][2(3/2)]\}$	3^-
$\{[1(-1/2)][1(-3/2)][1(3/2)]\}^{-1} \{[2(-5/2)][2(-3/2)][2(3/2)]\}$	2^-
$\{[1(-3/2)][1(-1/2)][1(1/2)]\}^{-1} \{[2(-5/2)][2(-3/2)][2(3/2)]\}$	1^-
$\{[1(3/2)][1(-1/2)][1(1/2)]\}^{-1} \{[2(3/2)][2(-5/2)][2(5/2)]\}$	3^-
$\{[1(1/2)][1(-3/2)][1(3/2)]\}^{-1} \{[2(-3/2)][2(-5/2)][2(5/2)]\}$	2^-
$\{[1(-1/2)][1(-3/2)][1(3/2)]\}^{-1} \{[2(-3/2)][2(-5/2)][2(5/2)]\}$	1^-
$\{[1(-3/2)][1(-1/2)][1(1/2)]\}^{-1} \{[2(-3/2)][2(-5/2)][2(5/2)]\}$	0^-

Thus, the 3p-3h states have parity $\pi=-1$ and are $(\pm 4)^-, (\pm 3)^-, (\pm 2)^-, (\pm 1)^-$, for a single population of the $[2(\pm 5/2)]$ state, and $(\pm 3)^-, (\pm 2)^-, (\pm 1)^-, 2(0^-)$ for a single population of the $[2(\pm 3/2)]$ state. So, for the $(3p3h)_{12}^-$ multiplet, there are all together 8 doubly-degenerate negative-parity states at an excitation energy $E_x = 9\epsilon_0$: $\{4^-, 2(3^-), 2(2^-), 2(1^-), 0^-\}$.

6. $[(2p2h)_{12\nu}(1p1h)_{12p}]^-$ multiplet at $E_x = 9\epsilon_0$ involving three identical nucleons

As one observes in Table IV, the $(2p2h)_{12\nu}$ states consists of a set of 18 doubly-degenerate states with spin and parity: $\{6^+, 5^+, 2(4^+), 2(3^+), 4(2^+), 5(1^+), 3(0^+)\}$. The $(1p1h)_{12p}$ states consists of a set of 8 doubly-degenerate states with spin and parity: $\{0, 2(1), 2(2), 2(3), 4\}$. They can be combined independently as in table XIV.

TABLE XIV. The spin states of the $[(2p2h)_{12\nu}(2p2h)_{02p}]^+$ multiplet at $E_x = 14\epsilon_0$. The parities of these states are all negative.

$[(2p2h)_{12p}]$ State	$[(2p2h)_{12\nu}]$ State						
	6	5	2(4)	2(3)	4(2)	5(1)	3(0)
4	10	9	2(8)	2(7)	4(6)	5(5)	3(4)
2(3)	2(9)	2(8)	4(7)	4(6)	8(5)	10(4)	6(3)
2(2)	2(8)	2(7)	4(6)	4(5)	8(4)	10(3)	6(2)
2(1)	2(7)	2(6)	4(5)	4(4)	8(3)	10(2)	6(1)
0	6	5	2(4)	2(3)	4(2)	5(1)	3(0)
0	6	5	2(4)	2(3)	4(2)	5(1)	3(0)
2(-1)	2(5)	2(4)	4(3)	4(2)	8(1)	10(0)	6(-1)
2(-2)	2(4)	2(3)	4(2)	4(1)	8(0)	10(-1)	6(-2)
2(-3)	2(3)	2(2)	4(1)	4(0)	8(-1)	10(-2)	6(-3)
-4	2	1	2(0)	2(-1)	4(-2)	5(-3)	3(-4)

The table consists of the set of negative parity states:

$\{10^-, 3(9^-), 6(8^-), 10(7^-), 16(6^-), 25(5^-), 33(4^-), 36(3^-), 35(2^-), 33(1^-), 30(0^-), 26(-1)^-, 20(-2)^-, 11(-3)^-, 3(-4)^-\}$. The other complimentary case gives the same set except with the sign of I_z reversed. Combining the two sets gives the final set of doubly-degenerate states in the $[(2p2h)_{12\nu}(2p2h)_{02p}]^+$ multiplet at $E_x = 14\epsilon_0$ comprising of 288 doubly-degenerate states of $\{10^-, 3(9^-), 6(8^-), 10(7^-), 16(6^-), 25(5^-), 36(4^-), 47(3^-), 55(2^-), 59(1^-), 30(0^-)\}$.

7. $[(2p2h)_{12}(1p1h)_{02}]^+$ multiplet at $E_x = 10\epsilon_0$ involving identical nucleons

The final state has three nucleons in the $\Lambda_z = 2$ shell. We combine all three particles and all three holes separately following the Pauli principle. The three particles behave as a single particle in that shell, with spins $\pm 3/2$ and $\pm 5/2$: $\{5/2, 3/2, -3/2, -5/2\}$. Next, we combine the three holes: one in the $\Lambda = 0$ shell, and the other two in the $\Lambda_z = 1$ shell. The two holes in $\Lambda_z = 1$ shell combine together to form spin $\{2, 1, 0, 0, -1, -2\}$ while the hole in the $\Lambda_z = 0$ shell has spin $\{1/2, -1/2\}$. We combine the spin of the three holes in the following table:

TABLE XV. The two holes in $\Lambda_z = 2$ combined with 1 hole in $\Lambda_z = 0$ shell gives spins in this table

two holes in $\Lambda_z = 1$ shell	one hole in $\Lambda = 0$ shell	
	1/2	-1/2
2	5/2	3/2
1	3/2	1/2
0	1/2	-1/2
0	1/2	-1/2
-1	-1/2	-3/2
-2	-3/2	-5/2

For the $[(1p1h)_{12}(2p2h)_{02}]^+$ multiplet at $E_x = 10\epsilon_0$, the three hole states combine to form states with spin $\{5/2, 2(3/2), 3(1/2), 3(-1/2), 2(-3/2), -5/2\}$. Now combine the three hole states with the three particle states, we get the spin configurations of the $[(1p1h)_{12}(2p2h)_{02}]^+$ multiplet in Table XVI.

TABLE XVI. The spin states of the $[(1p1h)_{02}(2p2h)_{12}]^+$ multiplet at $E_x = 10\epsilon_0$. The three particles in $\Lambda = 2$ shell combine with the three holes (one hole in the $\Lambda_z = 1$ shell combined with two holes in the $\Lambda_z = 0$ shell) gives spins in this table. All states in the $[(1p1h)_{02}(2p2h)_{12}]^+$ multiplet have a negative parity.

$[(1p1h)_{02}(2p2h)_{12}]^+$ State three particles in $\Lambda_z = 2$ shell				
two holes in $\Lambda_z = 1$ shell and one hole in $\Lambda_z = 0$ shell	5/2	3/2	-3/2	-5/2
5/2	5	4	1	0
2(3/2)	2(4)	2(3)	2(0)	2(-1)
3(1/2)	3(3)	3(2)	3(-1)	3(-2)
3(-1/2)	3(2)	3(1)	3(-2)	3(-3)
2(-3/2)	2(1)	2(0)	2(-3)	2(-4)
-5/2	0	-1	-4	-5

From Table XVI, we find that the $[(1p1h)_{02}(2p2h)_{12}]^+$ multiplet at $E_x = 10\epsilon_0$ comprises of 24 doubly-degenerate positive parity states: $\{5^+, 3(4^+), 5(3^+), 6(2^+), 6(1^+), 3(0^+)\}$.

8. $[(2p2h)_{12p}(1p1h)_{02\nu}]^-$ multiplet at $E_x = 10\epsilon_0$ involving different nucleons

As one observes in Table IV, the $(2p2h)_{12p}$ states consists of a set of 18 doubly-degenerate states with spin and parity: $\{6^+, 5^+, 2(4^+), 2(3^+), 4(2^+), 5(1^+), 3(0^+)\}$. The $(1p1h)_{02\nu}$ states consists of a set of 4 doubly-degenerate states with spin and parity: $\{1^+, 2(2^+), 3^+\}$. They can be combined independently as in table XVII.

TABLE XVII. The spin states of the $[(1p1h)_{02\nu}(2p2h)_{12p}]^+$ at $E_x = 10\epsilon_0$. The parities of these states are all negative.

$[(2p2h)_{12p}]$ State	$[(2p2h)_{12\nu}]$ State						
	6	5	2(4)	2(3)	4(2)	5(1)	3(0)
3	9	8	2(7)	2(6)	4(5)	5(4)	3(3)
2(2)	2(8)	2(7)	4(6)	4(5)	8(4)	10(3)	6(2)
1	7	6	2(5)	2(4)	4(3)	5(2)	3(1)
-1	5	4	2(3)	2(2)	4(1)	5(0)	3(-1)
2(-2)	2(4)	2(3)	4(2)	4(1)	8(0)	10(-1)	6(-2)
-3	3	2	2(1)	2(0)	4(-1)	5(-2)	3(-3)

The table consists of the set of 144 negative parity states: $\{9^+, 3(8^+), 5(7^+), 7(6^+), 11(5^+), 18(4^+), 22(3^+), 18(2^+), 13(1^+), 15(0^+), 17(-1)^+, 11(-2)^+, 3(-3)^+\}$. The other complimentary case gives the same set except with the sign of I_z reversed. Combining the two sets gives the the $[(1p1h)_{02\nu}(2p2h)_{12p}]^+$ multiplet at $E_x = 10\epsilon_0$ comprising of 144 doubly-degenerate positive parity states

of $\{9^+, 3(8^+), 5(7^+), 7(6^+), 11(5^+), 18(4^+), 25(3^+), 29(2^+), 30(1^+), 15(0^+)\}$.

9. $[(2p2h)_{02}(1p1h)_{12}]^+$ multiplet at $E_x = 11\epsilon_0$ involving identical nucleons

The final state has three nucleons in the $\Lambda_z = 2$ shell. We combine all three particles and all three holes separately following the Pauli principle. The three particles behave as a single particle in that shell, with spin $\pm 3/2$ and $\pm 5/2$: $\{5/2, 3/2, -3/2, -5/2\}$. Next, we combine the three holes: one in the $\Lambda_z = 1$ shell, and the other two in the $\Lambda_z = 0$ shell. The two holes in the $\Lambda_z = 0$ shell combine together to form spin $\{0\}$ while the hole in the $\Lambda_z = 1$ shell has spin $\{3/2, 1/2, -1/2, -3/2\}$.

TABLE XVIII. The spin states of the $[(1p1h)_{02}(2p2h)_{12}]^+$ multiplet at $E_x=11\epsilon_0$. The three particles in $\Lambda = 2$ shell combine with the three holes (2 holes in the $\Lambda_z = 1$ shell combined with 1 hole in the $\Lambda_z = 0$ shell) give spins in this table. All states in the $[(1p1h)_{02}(2p2h)_{12}]^+$ multiplet have a positive parity.

[[1p1h] ₁₂ (2p2h) ₀₂] ⁺ state three particles in $\Lambda_z = 2$ shell				
two holes in $\Lambda_z = 0$ shell and one hole in $\Lambda_z = 1$ shell	5/2	3/2	-3/2	-5/2
3/2	4	3	0	-1
1/2	3	2	-1	-2
-1/2	2	1	-2	-3
-3/2	1	0	-3	-4

From Table XVIII, we find that the $[(1p1h)_{02}(2p2h)_{12}]^+$ multiplet at $E_x = 10\epsilon_0$ comprises of 8 doubly-degenerate states: $\{4^-, 2(3^-), 2(2^+), 2(1^-), 0^-\}$.

10. $(4p4h)_{12}^+$ multiplet at $E_x=12\epsilon_0$ involving four identical nucleons

In making the (4 particle)-(4 hole) excitation from the $\Lambda=1$ shell to the $\Lambda=2$ shell the four identical nucleons complete a closed shell configuration with the full occupation of the $\Lambda = 2$ shell, at an excitation energy $E_x = 12\epsilon_0$.

TABLE XIX. $(4p4h)_{12}^+$ ($\Lambda=1$) \rightarrow ($\Lambda=2$) excitations at $E_x=4\Delta_{12}=12\epsilon_0$ involving four identical particles

(4 particle)-(4 hole) configuration	I^π
$\{[1(3/2)][1(-3/2)][1(-1/2)][1(1/2)]\}^{-1}$	0^+
$\{[2(-5/2)][2(5/2)][2(-3/2)][2(3/2)]\}$	

11. $[(2p2h)_{12\nu}(2p2h)_{12p}]^+$ multiplet at $E_x = 12\epsilon_0$

As one observes in Table IV, the $(2p2h)_{12}$ states consists of a set of 18 doubly-degenerate states with spin and parity $\{6^+, 5^+, 2(4^+), 2(3^+), 4(2^+), 5(1^+), 3(0^+)\}$. The multiplet $[(2p2h)_{12\nu}(2p2h)_{12p}]^+$ involving two neutrons and two protons can combine their multiplet states independently as in table XX.

TABLE XX. The spin states of the $[(2p2h)_{12\nu}(2p2h)_{12p}]^+$ at $E_x=12\epsilon_0$ gives spins in this table. All these states have a positive parity.

[(2p2h) _{12ν} states	[(2p2h) _{12p} state						
	6	5	2(4)	2(3)	4(2)	5(1)	3(0)
6	12	11	2(10)	2(9)	4(8)	5(7)	3(6)
5	11	10	2(9)	2(8)	4(7)	5(6)	3(5)
2(4)	2(10)	2(9)	4(8)	4(7)	8(6)	10(5)	6(4)
2(3)	2(9)	2(8)	4(7)	4(6)	8(5)	10(4)	6(3)
4(2)	4(8)	4(7)	8(6)	8(5)	16(4)	20(3)	12(2)
5(1)	5(7)	5(6)	10(5)	10(4)	20(3)	25(2)	15(1)
3(0)	3(6)	3(5)	6(4)	6(3)	12(2)	15(1)	9(0)
3(0)	3(6)	3(5)	6(4)	6(3)	12(2)	15(1)	9(0)
5(-1)	5(5)	5(4)	10(3)	10(2)	20(1)	25(0)	15(-1)
4(-2)	4(4)	4(3)	8(2)	8(1)	16(0)	20(-1)	12(-2)
2(-3)	2(3)	2(2)	4(1)	4(0)	8(-1)	10(-2)	6(-3)
2(-4)	2(2)	2(1)	4(0)	4(-1)	8(-2)	10(-3)	6(-4)
(-5)	(1)	(0)	2(-1)	2(-2)	4(-3)	5(-4)	3(-5)
(-6)	(0)	(-1)	2(-2)	2(-3)	4(-4)	5(-5)	3(-6)

We collect all spin states, and get the set: $\{12^+, 2(11^+), 5(10^+), 8(9^+), 16(8^+), 26(7^+), 39(6^+), 50(5^+), 63(4^+), 74(3^+), 83(2^+), 80(1^+), 69(0^+), 50(-1^+), 34(-2^+), 22(-3^+), 15(-4^+), 8(-5^+), 3(-6^+)\}$. The other complementary case case with negative I_z of the $(2p2h)_{12p}$ multiplet gives the same set with the sign of I_z reversed. So, the $[(2p2h)_{12\nu}(2p2h)_{12p}]^+$ multiplet at $E_x=12\epsilon_0$ comprises of 648 doubly-degenerate states of the set:

$\{12^+, 2(11^+), 5(10^+), 8(9^+), 16(8^+), 26(7^+), 42(6^+), 58(5^+), 78(4^+), 96(3^+), 117(2^+), 130(1^+), 69(0^+)\}$.

12. $[(3p3h)_{12}(1p1h)_{02}]^-$ multiplet at $E_x = 13\epsilon_0$ involving identical nucleons

The four particles in the $\Lambda_z=2$ complete a closed shell and have $I_z=0$. The three holes in the $\Lambda_z=1$ shell have spins $\{3/2, 1/2, -1/2, -3/2\}$ and the hole in the $\Lambda_z=0$ shell has spins $\{1/2, -1/2\}$. As in Table VIII, the $[(3p3h)_{12}(1p1h)_{02}]^+$ multiplet at $E_x = 13\epsilon_0$ involving identical nucleons form the set of 4 doubly-degenerate states $\{2^-, 2(1^-), 0^-\}$.

13. $[(3p3h)_{12\nu}(1p1h)_{02p}]^-$ multiplet at $E_x = 13\epsilon_0$ involving three neutrons and one proton

The $(3p3h)_{12\nu}$ multiplet contains 8 doubly-degenerate states $\{4^-, 2(3^-), 2(2^-), 2(1^-), 0^-\}$ and the $(1p1h)_{02p}$ multiple contains 4 doubly-degenerate states $\{3^+, 2(2^+), 1^+\}$. The $[(3p3h)_{12\nu}(1p1h)_{02p}]^-$ at $E_x = 13\epsilon_0$ involving three neutrons and one proton contains 64 doubly-degenerate states: $\{7^-, 4(6^-), 7(5^-), 8(4^-), 9(3^-), 12(2^-), 15(1^-), 8(0^-)\}$.

14. $[(2p2h)_{02}(2p2h)_{12}]^+$ multiplet at $E_x = 14\epsilon_0$ involving identical nucleons

The four particles in the $\Lambda_z=2$ shell completes a closed shell and a total spin $I_z=0$. It is only necessary to find the I_z of the two holes in the $\Lambda_z=0$ and two holes in the $\Lambda_z = 2$ shells. The two holes in the $\Lambda_z=0$ complete a closed shell, and have a total spin of $I_z=0$. The two holes in the $\Lambda_z=1$ shell have spins $\{2, 1, 0, 0, -1, -2\}$, so the $[(2p2h)_{02}(2p2h)_{12}]^+$ multiplet at $E_x = 14\epsilon_0$ contains 3 doubly-degenerate states: $\{2^+, 1^+, 0^+\}$.

15. $[(2p2h)_{12\nu}(2p2h)_{02p}]^+$ multiplet at $E_x = 14\epsilon_0$

The $(2p2h)_{12\nu}$ multiplet contains a set of 18 doubly-degenerate states with spin and parity

$\{6^+, 5^+, 2(4^+), 2(3^+), 4(2^+), 5(1^+), 3(0^+)\}$. The $(2p2h)_{02p}$ states contains a set of 3 doubly-degenerate states with spin and parity $\{0^+, 1^+, 4^+\}$. Combining these two sets of states, we get the spins of the multiplet in table XXI.

TABLE XXI. The spin states of the $[(2p2h)_{12\nu}(2p2h)_{02p}]^+$ multiplet at $E_x = 14\epsilon_0$. All these states have a positive parity.

[[$(2p2h)_{02p}$ State	[[$(2p2h)_{12\nu}$ State						
	6	5	2(4)	2(3)	4(2)	5(1)	3(0)
4	10	9	2(8)	2(7)	4(6)	5(5)	3(4)
1	7	6	2(5)	2(4)	4(3)	5(2)	3(1)
0	6	5	2(4)	2(3)	4(2)	5(1)	3(0)
0	6	5	2(4)	2(3)	4(2)	5(1)	3(0)
-1	5	4	2(3)	2(2)	4(1)	5(0)	3(-1)
-4	2	1	2(0)	2(-1)	4(-2)	5(-3)	3(-4)

This table contains of set of states: $\{10^+, 9^+, 2(8^+), 3(7^+), 7(6^+), 10(5^+), 10(4^+), 10(3^+), 16(2^+), 18(1^+), 13(0^+), 5(-1^+), 4(-2^+), 5(-3^+), 3(-4^+)\}$. The other complimentary case gives the same set except with the sign of I_z reversed. Combine the complementary set, we find that the $[(2p2h)_{12\nu}(2p2h)_{02p}]^+$ multiplet at $E_x = 14\epsilon_0$ contains 108 doubly-degenerate positive parity states of the set: $\{10^+, 9^+, 2(8^+), 3(7^+), 7(6^+), 13(5^+), 10(4^+), 15(3^+), 20(2^+), 23(1^+), 13(0^+)\}$.

-
- [1] J. A. Wheeler, *Molecular Viewpoint in nuclear structure*, Phys. Rev. **52**, 1083 (1937).
[2] J. A. Wheeler, *On the Mathematical Description of Light Nuclei by the Method of Resonating Group Structure*, Phys. Rev. **52**, 1107 (1937).
[3] D. N. F. Dunbar, R. E. Pixley, W.A. Wenzel, and W. Whaling, *The 7.68-MeV state in C^{12}* , Phys. Rev. **92**, 649 (1953).
[4] F. Hoyle, D. N. F. Dunbar, W.A. Wenzel, and W. Whaling, Phys. Rev. **92**, 1095c (1953).
[5] F. Hoyle, *On nuclear reaction occuring in very hot stars*, Astrophys. J. Supplement, **51**, 121 (1954).
[6] C. W. Cook, W. A. Fowler, and T. Lauritsen, Phys. Rev. **107**, 508 (1957).
[7] C. Wheldon, Tz. Kokalova, M. Freer, A. Glenn, D. J. Parker, T. Roberts, and I. Walmsley *States at high excitation in ^{12}C from the $^{12}C(^3He, ^3He)3\alpha$ reaction*, Phys. Rev. **C90**, 014319 (2014).
[8] T. K. Wheldon, *Over half a century of studying carbon-12*, J. Phys.: Conf. Ser. **639**, 012003 (2015).
[9] R. Smith *et al.*, *New Measurement of the Direct 3α Decay from the ^{12}C Hoyle State*, Phys. Rev. Lett. **119**, 132502 (2017).
[10] D. Dell'Aquila *et al.*, *High-Precision Probe of the Fully Sequential Decay Width of the Hoyle State in ^{12}C* , Phys. Rev. Lett. **119**, 132501 (2017).
[11] W. R. Zimmerman *et al.*, *Unambiguous Identification of the Second 2^+ State in ^{12}C and the Structure of the Hoyle State*, Phys. Rev. Lett. **110**, 152502 (2013).
[12] M. Gai, *Current and Future Tests of the Algebraic Cluster Model of ^{12}C* , J. Phys. Conf. Ser. **876**, 012009 (2017).
[13] J.H. Kelley, J.E. Purcell, C.G. Sheu, *Energy levels of light nuclei $A = 12$* , Nucl. Phys. **A 968**, 71253 (2017).
[14] O. S. Kirsebom, M. Alcorta, M. J. G. Borge, M. Cubero, C. A. Diget, R. Dominguez-Reyes, L. M. Fraile, B. R. Fulton, H. O. U. Fynbo, S. Hyldegaard, B. Jonson, M. Madurga, A. Muoz Martin, T. Nilsson, G. Nyman, A. Perea, K. Riisager, and O. Tengblad, *Breakup of ^{12}C resonances into three α particles*, Phys. Rev. **C81**, 064313 (2010).
[15] O. S. Kirsebom, M. Alcorta, M. J. G. Borge, M. Cubero, C. A. Diget, L. M. Fraile, B. R. Fulton, H. O. U. Fynbo, D. Galaviz, B. Jonson, M. Madurga, T. Nilsson, G. Nyman, K. Riisager, O. Tengblad, and M. Turrión, *Improved Limit on Direct α Decay of the Hoyle State*, Phys. Rev.Lett. **108**, 202501 (2012).
[16] Alcorta *et al.*, *Properties of ^{12}C resonances determined from the $^{10}B(^3He, p\alpha\alpha\alpha)$ and $^{11}B(^3He, d\alpha\alpha\alpha)$ reactions studied in complete kinematics*, Phys. Rev. **C81**, 064306 (2012).
[17] M. Barbui, K. Hagel, J. Gauthier, S. Wuenschel, R. Wada, V. Z. Goldberg, R. T. deSouza, S. Hudan, D. Fang, X.-G. Cao, and J. B. Natowitz, *Searching for states analogous to the ^{12}C Hoyle state in heavier nuclei using*

- the thick target inverse kinematics technique*, Phys. Rev. **C98**, 044601 (2018).
- [18] D. M. Brink, in Proc. Int. School of Physics“Enrico Fermi”, Course XXXVI, Varenna, 1965 ed C Bloch (New York: Academic Press), 1966, p. 247.
- [19] R. Álvarez-Rodríguez, A. S. Jensen, D. V. Fedorov, H. O. U. Fynbo, E. Garrido *Energy Distributions from Three-Body Decaying Many-Body Resonances*, Phys. Rev. Lett. **99**, 072503 (2007).
- [20] R. Alvarez-Rodríguez, A. S. Jensen, E. Garrido, D. V. Fedorov, and H. O. U. Fynbo, *Momentum distributions of particles from decaying low-lying ^{12}C resonances*, Phys. Rev. **C 77**, 064305 (2008).
- [21] H. O. U. Fynbo, R. Álvarez-Rodríguez, A. S. Jensen, O. S. Kirsebom, and D. V. Fedorov, E. Garrido, *Three-body decays and R-matrix analyses*, Phys. Rev. **C 79**, 054009 (2009).
- [22] S.G. Nilsson, *Binding states of individual nucleons in strongly deformed nuclei*, Mat. Fys. Medd., Dan. Vid. Selsk. **29** (1955).
- [23] C. Y. Wong, *Shells in a simple anisotropic harmonic oscillator*, Phys. Lett. **62B**, 668 (1970).
- [24] R. Bijker and F. Iachello, *The Algebraic Cluster Model: Three-Body Clusters*, Ann. Phys. (N.Y.) **298**, 334 (2002).
- [25] D.J. Marín-Lámbarrí, R. Bijker, M. Freer, M. Gai, Tz. Kokalova, D.J. Parker, and C. Wheldon, *Evidence for Triangular D_{3h} Symmetry in ^{12}C* , Phys. Rev. Lett. **113**, 012502 (2014).
- [26] W. von Oertzen, Z. Phys. **A 354**, 37 (1996); W. von Oertzen, M. Freer and Y. Kanada-En'yo, Phys. Rep. **432**, 43 (2006).
- [27] Y. Kanada-En'yo and H. Horiuchi, *Structure of Light Unstable Nuclei Studied with Antisymmetrized Molecular Dynamics*, Prog. of Theo. Phys. Suppl. **142** 205 (2001).
- [28] Y. Kanada-En'yo, *The Structure of Ground and Excited States of ^{12}C* , Prog. of Theo. Phys. **117** 655 (2007).
- [29] R. Roth, T. Neff, H. Hergert and H. Feldmeier, Nucl. Phys. **A 745**, 3 (2004).
- [30] M. Chernykh, H. Feldmeier, T. Neff, P. von Neumann-Cosel, and A. Richter, *Structure of the Hoyle State in ^{12}C* , Phys. Rev. Lett. **98**, 032501 (2007).
- [31] Y. Funaki, H. Horiuchi, W. von Oertzen, G. Ropke, P. Schuck, A. Tohsaki, and T. Yamada, *Concepts of nuclear α -particle condensation*, Phys. Rev. **C 80**, 064326 (2009), and references therein, M. Kamimura, Nucl. Phys. **A351**, 456 (1981).
- [32] R. Roth, J. Langhammer, A. Calci, S. Binder, and P. Navratil, *Similarity-Transformed Chiral $NN+3N$ Interactions for the Ab Initio Description of ^{12}C and ^{16}O* , Phys. Rev. Lett. **107**, 072501 (2011).
- [33] B.R. Barrett, P. Navratil and J.P. Vary, Prog. Part. Nucl. Phys. **69**, 131 (2013).
- [34] A. C. Dreyfuss, K. D. Launey, T. Dytrych, J. P. Draayer, and C. Bahri, *Hoyle state and rotational features in Carbon-12 within a no-core shell model framework*, Phys. Lett. **B 727**, (2013), pp. 511-515.
- [35] E. Epelbaum, H. Krebs, D. Lee, and U.-G. Meissner, *Ab Initio Calculation of the Hoyle State*, Phys. Rev. Lett. **106**, 192501 (2011).
- [36] M. Freer, H. Horiuchi, Y. Kanada-En'yo, D. Lee, and U.-G. Meiner, *Microscopic Clustering in Nuclei*, arXiv:1705.06192.
- [37] J. L. Egido and L. M. Robledo, Nucl. Phys. **A 738**, 31 (2004).
- [38] P. Arumugam, B.K. Sharma, S.K. Patra, R.K. Gupta, Phys. Rev. **C 71**, 064308 (2005).
- [39] P.-G. Reinhard, J. A. Maruhn, A. S. Umar, and V. E. Oberacker, Phys. Rev. **C 83**, 034312 (2011).
- [40] J.-P. Ebran, E. Khan, T. Niki, and D. Vretenar, *How atomic nuclei cluster*, Nature **487**, 341 (2012); J.-P. Ebran, E. Khan, T. Niki, and D. Vretenar, *Density functional theory studies of cluster states in nuclei*, Phys. Rev. **C 90**, 054329 (2014); J.-P. Ebran, E. Khan, T. Niki, and D. Vretenar, Jour. Phys. G **44**, 103001 (2017).
- [41] T. Ichikawa, J. A. Maruhn, N. Itagaki, and S. Ohkubo, Phys. Rev. Lett. **107**, 112501 (2011); Y. Iwata, T. Ichikawa, N. Itagaki, J. A. Maruhn, and T. Otsuka, Phys. Rev. **C 92**, 011303 (2015); J. M. Yao, N. Itagaki, and J. Meng, Phys. Rev. **C 90**, 054307 (2014).
- [42] P. W. Zhao, N. Itagaki, and J. Meng, Phys. Rev. Lett. **115**, 022501 (2015); E. F. Zhou, J. Yao, Z. Li, J. Meng, and P. Ring, Phys. Lett. **B 753**, 227 (2016);
- [43] A. V. Afanasjev and H. Abusara, Phys. Rev. **C 97**, 024329 (2018).
- [44] A. Staszczak and C. Y. Wong, (to be published).
- [45] Y. Suzuki, H. Horiuchi, and K. Ikeda, Prog. Theor. Phys. **47**, 1517 (1972).
- [46] Z. X. Ren, S. Q. Zhang, P. W. Zhao, N. Itagaki, J. A. Maruhn, and J. Meng, arXiv:1805.07901.
- [47] T. Inakura and S. Mizutori, *Rod-shaped rotational states in $N=Z$ even-even nuclei from ^{12}C to ^{32}S* , Phys. Rev. **C 98**, 044312 (2018).
- [48] C. Y. Wong, *Toroidal nuclei*, Phys. Lett. **41B**, 446-450 (1972)
- [49] C. Y. Wong. *Toroidal and spherical bubble nuclei*, Ann. of Phys. (N.Y.) **77**, 279 (1973).
- [50] M. Brack, J. Damgaard, A. S. Jensen, H. C. Pauli, V. Strutinsky, and C. Y. Wong, *Funny Hills: The Shell-Correction Approach to Nuclear Shell Effects and Its Applications to the Fission Process*, Rev. Mod. Phys. **44**, 320-405 (1973).
- [51] X. G. Cao, E. J. Kim, K. Schmidt, K. Hagel, M. Barbui, J. Gauthier, S. Wuenschel, G. Giuliani, M. R. D. Rodriguez, S. Kowalski, H. Zheng, M. Huang, A. Bonasera, R. Wada, N. Blando, G. Q. Zhang, C. Y. Wong, A. Staszczak, Z. X. Ren, Y. K. Wang, S. Q. Zhang, J. Meng, and J. B. Natowitz, *Examination of Evidence for resonances at high excitation energy in the 7α disassembly of ^{28}Si* , Phys. Rev. **C 99**, 014606 (2019), arxiv:1801.07366.
- [52] A. Staszczak and C. Y. Wong, *A region of high-spin toroidal isomers*, Phys.Lett. **B 738**, 401-404 ;arXiv:1312.3413
- [53] Wei Zhang, Hao-Zhao Liang, Shuang-Quan Zhang, Jie Meng, *Search for Ring-Like Nuclei under Extreme Conditions*, Chin. Phys. Lett., **27**, 102103 (2010).
- [54] T. Ichikawa et al., *Existence of exotic torus configuration in high-spin excited states of 40Ca* , Phys.Rev.Lett. **109** (2012) 232503; T. Ichikawa et al., *Pure collective precession motion of a high-spin torus isomer*, Phys.Rev. **C90**, 034314 (2014).
- [55] T. Ichikawa, K. Matsuyanagi, J. A. Maruhn, N. Itagaki, *High-spin torus isomers and their precession motions* Phys.Rev. **C90**, 034314 (2014).
- [56] A. Staszczak and C. Y. Wong, *Particle-hole Nature of the Light High-spin Toroidal Isomers*, Acta Phys.Polon. **B46**, no.3, 675 (2015); arXiv:1504.07646 [nucl-th]
- [57] A. Staszczak and C. Y. Wong, *Toroidal high-spin isomers*

- in light nuclei with N not equal to Z* , Phys.Scripta **90**, (2015) 114006; arXiv:1412.0050 [nucl-th]
- [58] A. Staszczak and C. Y. Wong, *Theoretical studies of possible toroidal high-spin isomers in the light-mass region*, EPJ Web Conf. **117**, 04008 (2016), arXiv:1510.04610.
- [59] G. A. Grin, C. Joseph, C. Y. Wong, and T. Tamura, *Scattering of 14.1 MeV Neutrons from ^{12}C* , Phys. Lett. **25B**, 387 (1967).
- [60] C. Y. Wong and A. Staszczak, *Shells in Toroidal Nuclei in the Intermediate Mass Region*, Phys. Rev. **C98**, 034316 (2018).
- [61] A. Bohr and B. Mottelson, *Nuclear Structure*, Vol I. W.A.Benjamin, Inc, N.Y. 1969
- [62] K. Hara and Y. Sun, *Projected Shell Model and High Spin-Spectroscopy*, Int. J. Mod. Phys. **E 4**, 637 (1995).
- [63] Y. Sun and C. L. Wu, *Multishell shell model for heavy nuclei*, Physical Review **C 68**, 024315 (2003).
- [64] Y. Sun, *Projected shell model study on nuclei near the $N = Z$ line*, Eur. Phys. J. **A20**, 133-138 (2004), arXiv:nucl-th/0211043v2.
- [65] Y. Sun, *Projected shell model description for nuclear isomers*, Rev. Mex. Fis. Suppl. **54**, 01122 (2008), arXiv:0803.1700 [nucl-th]
- [66] M. Alcorta, O. Kirsebom, M.J.G. Borge, H.O.U. Fynbo, K. Riisager, O. Tengblad, *A complete kinematics approach to study multi-particle final state reactions*, Nucl. Instrum. Methods **A 605**, 318 (2009).
- [67] A. Kosior, A. Staszczak, C. Y. Wong, *Superheavy toroidal nuclei in the Skyrme energy functional framework*, Acta Phys. Pol. B Proc. Suppl. **10**, 249 (2017), [arXiv:1701.06327]
- [68] A. Staszczak, C. Y. Wong, A. Kosior, *Toroidal high-spin isomers in the nucleus $^{304}120$* Phys. Rev. **C 95**, 054315 (2017) [arXiv:1705.01408]
- [69] O. S. Kirsebom, *Decay of $^{12}\text{C}^*$ into three α particles*, Few-Body Syst. **54**, 755 (2013).
- [70] M. Freer, S. Almaraz-Calderon, A. Aprahamian, N. I. Ashwood, M. Barr, B. Bucher, P. Copp, M. Couder, N. Curtis, X. Fang, F. Jung, S. Leshner, W. Lu, J. D. Malcolm, A. Roberts, W. P. Tan, C. Wheldon, and V. A. Ziman *Evidence for a new 12C state at 13.3 MeV*, Phys. Rev. **C 83**, 034314 (2011).
- [71] E. Garrido, A.S. Jensen, D.V. Fedorov, *Three-body bremsstrahlung and the rotational character of the 12C -spectrum*, Phys. Rev. **bf C91**, 054003 (2015)